Stem Cell Reports
Article

OPEN ACCESS

The POU/Oct Transcription Factor Nubbin Controls the Balance of Intestinal Stem Cell Maintenance and Differentiation by Isoform-Specific Regulation

Xiongzhuo Tang,[1] Yunpo Zhao,[1] Nicolas Buchon,[2] and Ylva Engström[1,*]
[1]Department of Molecular Biosciences, The Wenner-Gren Institute, Stockholm University, Stockholm 10691, Sweden
[2]Department of Entomology, Cornell University, Ithaca, NY 14853, USA
*Correspondence: ylva.engstrom@su.se
https://doi.org/10.1016/j.stemcr.2018.03.014

SUMMARY

Drosophila POU/Oct transcription factors are required for many developmental processes, but their putative regulation of adult stem cell activity has not been investigated. Here, we show that Nubbin (Nub)/Pdm1, homologous to mammalian OCT1/POU2F1 and related to OCT4/POU5F1, is expressed in gut epithelium progenitor cells. We demonstrate that the *nub*-encoded protein isoforms, Nub-PB and Nub-PD, play opposite roles in the regulation of intestinal stem cell (ISC) maintenance and differentiation. Depletion of Nub-PB in progenitor cells increased ISC proliferation by derepression of *escargot* expression. Conversely, loss of Nub-PD reduced ISC proliferation, suggesting that this isoform is necessary for ISC maintenance, analogous to mammalian OCT4/POU5F1 functions. Furthermore, Nub-PB is required in enteroblasts to promote differentiation, and it acts as a tumor suppressor of Notch RNAi-driven hyperplasia. We suggest that a dynamic and well-tuned expression of Nub isoforms in progenitor cells is required for maintaining gut epithelium homeostasis.

INTRODUCTION

Adult stem cells exhibit the ability to replace damaged and aged cells during normal epithelium regeneration as well as in response to injury and cellular stress, thereby maintaining tissue homeostasis. The mammalian adult gut epithelium contains intestinal stem cells (ISCs), which are located in crypts along the small intestine where they frequently proliferate to retain homeostatic status (Barker et al., 2008). Proper ISC activities play a pivotal role in the maintenance of cellular homeostasis in the intestine. Dysfunctional ISC proliferation and/or differentiation in the gut epithelium are associated with chronic diseases and developmental abnormalities, such as inflammatory bowel diseases, dysplasia, and metaplasia (Li and Jasper, 2016). However, the mechanisms that maintain gut homeostasis are still largely unknown. The *Drosophila* midgut shares many similarities with the mammalian small intestine in terms of organ structure and function. Genetic manipulation of evolutionarily conserved signaling pathways linked to ISC proliferation and differentiation in the *Drosophila* midgut has become a favorable model for investigations of ISC activities and the underlying mechanisms controlling epithelial regeneration and homeostasis (Apidianakis and Rahme, 2011; Bergman et al., 2017; Liu et al., 2017).

Drosophila ISCs are derived from adult midgut precursors during larval stages, and thereafter reside in the midgut basal epithelium (Micchelli, 2012; Micchelli and Perrimon, 2006). The ISC lineage is controlled by bidirectional Notch signaling in the daughter cells. A daughter cell with a high level of Notch activity becomes an intermediate enteroblast (EB), which further differentiates into an enterocyte (EC). Low degree of Notch activity results in retained ISC identity and, in combination with strong *Delta* and *Prospero* expression, the daughter cell is primed to differentiate into a pre-enteroendocrine (pre-EE) cell and further into an enteroendocrine (EE) cell (Biteau and Jasper, 2014; Guo and Ohlstein, 2015; Ohlstein and Spradling, 2006, 2007; Perdigoto et al., 2011; Zeng and Hou, 2015). Establishment and maintenance of the *Drosophila* gut epithelium require strict control of ISC proliferation and differentiation, and has to be balanced with cell death and delamination of differentiated ECs over time. Disruption of this cellular homeostasis can cause abnormal gut functionalities, such as tumor growth or increased susceptibility to infection (Amcheslavsky et al., 2009; Buchon et al., 2009; Ohlstein and Spradling, 2007; Patel et al., 2015). Both intrinsic and extrinsic signals contribute to maintain normal ISC activities via several evolutionarily conserved signal transduction pathways, such as Notch/Delta, Janus kinase/signal transducer and activator of transcription, Jun N-terminal kinase, epidermal growth factor receptor, bone morphogenetic proteins, Hippo, Slit/Robo, and their downstream transcription factors (Bardin et al., 2010; Biteau et al., 2008; Biteau and Jasper, 2014; Buchon et al., 2010; Dutta et al., 2015; Jiang et al., 2009; Korzelius et al., 2014; Ohlstein and Spradling, 2007; Ren et al., 2010; Tian and Jiang, 2014). Although these studies have endorsed a much better understanding of the processes that promote ISC proliferation, we still have rather limited knowledge about the mechanisms underlying the cellular homeostasis and how ISCs are maintained over a long period of time.

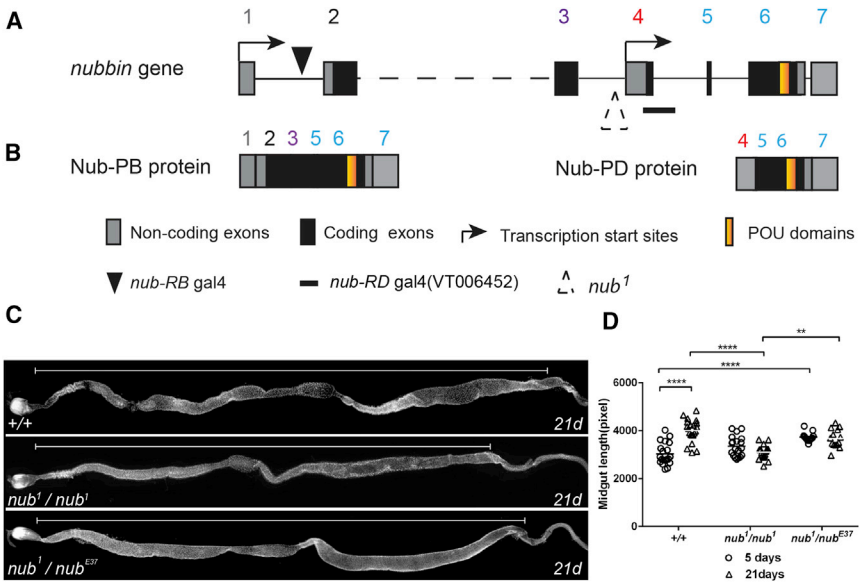

Figure 1. Midgut Length in Different *nub* Mutants during Adult Stages

(A) Schematic structure of the *Drosophila nub* gene. The *nub* gene contains seven exons, as depicted with boxes, and transcription is initiated at two separate promoters (arrows). Exons and introns (solid black line) are drawn to scale, except for the large intron between exon 2 and 3 (dashed line), which is reduced in size.

(B) Organization of Nub-PB and Nub-PD proteins encoded by the *nub* gene. Note that Nub-PB protein contains three unique exons (1, 2, and 3) while Nub-PD protein contains one unique exon (4). The shared three exons (5, 6, and 7) contain the coding sequence for the DNA-binding POU_S and POU_H domains (orange). Filled black triangle indicates the *nub-RB gal4* insertion site and black bold line shows the position of the *nub-RD-gal4* enhancer line. Two *nub* mutants, nub^1; 412 transposable element insertion site indicated by a dashed triangle in (A) and nub^{E37} (an EMS-induced null mutant for both Nub-PB and Nub-PD; Yeo et al., 1995) are used in this work.

(C) Midguts from 21-day-old control (top), nub^1/nub^1 (middle), and $nub^1/+$; nub^{E37} (bottom) flies.

(D) Measurement of midgut lengths in 5-day-old (circle) and 21-day-old (triangle) flies. Statistical significance was calculated using two-way ANOVA, Tukey's multiple comparisons test, $^{**}p < 0.01$, $^{****}p < 0.0001$. n = 13–21 guts. Error bars represent SEM.

The *nubbin (nub)/POU domain protein 1 (Pdm1)* gene is a member of the class II POU transcription factor family and shares homology with the OCT1/POU2F1 and OCT2/POU2F2 proteins in mammals (Holland et al., 2007; Tantin, 2013). The *nub* gene is also evolutionarily related to the class V POU factor OCT4/POU5F1, which maintains stemness of embryonic stem cells (ESCs) (Niwa et al., 2000), and is one of the crucial pluripotency factors used for reprogramming of differentiated cells to induced pluripotent stem cells (iPSCs) (Takahashi and Yamanaka, 2006). Alternative transcripts have earlier been reported to be expressed from the *nub* gene (Ng et al., 1995), and annotation of the *Drosophila* genome suggested at least two independent transcripts termed *nub-RB* and *nub-RD* (FlyBase: FBgn0085424). Recent experimental evidence has revealed that two protein isoforms, Nub-PB and Nub-PD, are expressed in *Drosophila* (Dantoft et al., 2013; Lindberg et al., 2018). Transcription of the *nub* gene initiates at two major promoters that are separated by more than 30 kB. The two transcripts *nub-RB* and *nub-RD* are translated into a large (Nub-PB; 103.9 kDa) and a small (Nub-PD; 65.2 kDa) isoform, respectively, with a common C-terminal part comprising the POU-specific (POU_S) and POU homeo (POU_H) DNA binding domains (Figures 1A and 1B).

We recently reported that Nub-PD is a transcriptional repressor of immune and stress response genes in the gut (Dantoft et al., 2013), and that loss of such repression leads to gut bacterial dysbiosis and short life span (Dantoft et al., 2016). Nub/Pdm1 immunostaining is robust in mature midgut ECs (Beebe et al., 2010; Lee et al., 2009; Mathur et al., 2010), and it was suggested that Nub-PD acts as a differentiation factor by repressing *escargot* (*esg*) expression (Korzelius et al., 2014). However, neither has a possible role of Nub-PB in regulation of intestinal stem cell activity been investigated, nor have the discrete roles and possible interplay between Nub-PB and Nub-PD in gut epithelium regeneration been analyzed.

Here, we report that Nub proteins are not only expressed in adult midgut ECs, but also present in progenitor cells (ISC + EB), and are necessary for maintaining cellular homeostasis during normal gut epithelium regeneration. Most importantly, we show that the two transcription factor isoforms, Nub-PB and Nub-PD, play opposite roles in regulating ISC maintenance and proliferation in the posterior midgut. Loss of Nub-PB leads to hyperplasia, as progenitor cells fail to differentiate and instead continue to proliferate. In contrast, Nub-PD mutant clones fail to proliferate, indicating that Nub-PD is necessary for the maintenance of ISCs. We suggest that this represents a mechanism to regulate adult stem cell activity with two transcription factor isoforms acting in opposite manners, one as a differentiation factor, the other as a stemness factor.

RESULTS

Loss of Nub-PD Restricts Midgut Length during Adult Life

To investigate whether *nub* is involved in regulation of adult gut homeostasis, the adult midgut length was measured in two different *nub* mutant fly strains, nub^{1} and nub^{E37}. The nub^{1} mutation eliminates expression of the Nub-PD isoform, while neither isoform is produced in nub^{E37} (Ng et al., 1995; Yeo et al., 1995). Dissected midguts of 21-day-old nub^{1} flies were clearly shorter than midguts of control flies (Figures 1C and 1D), indicating that Nub-PD is involved in development or regeneration of the adult midgut. To distinguish between defects during larval/pupal development from regeneration failure in adults, the midgut length was measured in young flies (5 days after eclosion). As expected, midguts derived from controls were shorter at day 5 compared with day 21 (Figure 1D), demonstrating that the midgut length normally increases between days 5 and 21. However, the midgut length of nub^{1} flies did not increase with age (Figure 1D). This indicates that the short midguts of nub^{1} flies at day 21 are not caused by early developmental effects, but rather due to failure in maintaining cellular homeostasis in the midgut. The nub^{E37} mutant is lethal during the pupal stage, while heteroallelic nub^{1}/nub^{E37} flies are viable. We used this combination to analyze whether Nub-PB is also involved in regulation of midgut length. Interestingly, loss of one copy of Nub-PB in the Nub-PD mutant background partly restored the midgut length at day 21 (Figure 1D), indicating that Nub-PB and Nub-PD may confer opposite roles in maintenance of midgut epithelial regeneration. Taken together, the changes in adult midgut length of different *nub* mutants suggest that both Nub isoforms are contributing to cellular homeostasis in the adult midgut.

Nub Is Expressed in Adult Midgut and in Cell Lines

Adult midgut ECs are recognized as large cells with polyploid nuclei, expressing *MyoIA* and marked by Nub antibody staining (Beebe et al., 2010; Jiang et al., 2009; Lee et al., 2009; Mathur et al., 2010). To reveal the specific expression of *nub-RB* and *nub-RD* transcripts, spatial expression of promoter-specific *nub-RB* and *nub-RD* reporter lines were analyzed. For analysis of *nub-RB* expression, a *MiMIC*-transgene ($nub^{MI05126}$) (Venken et al., 2011) (Figure 1A) was converted into a Gal4-expressing reporter and combined with *UAS-mCherry*. This reporter conferred robust staining throughout the adult midgut, overlapping with *MyoIA-lacZ*-positive ECs (Figures 2A–2A″ and S1A–S1A″). For *nub*-RD expression, a number of Vienna tiles enhancer lines (Kvon et al., 2014) were analyzed and the *VT6452 Gal4* line, which carries a 2.2-kB fragment including part of the first *nub-RD* exon and downstream intron sequences (Figure 1A), revealed strong reporter gene expression in adult midgut (Figures 2B–2B″ and S1B–S1B″). This demonstrates that both Nub-PB and Nub-PD are expressed in anterior and posterior midgut ECs. In addition, some cells with *nub-RB*- and *nub-RD*-driven mCherry expression were found to overlap with EBs, marked by the Notch activity reporter *GBE-Su(H)*-nlsGFP (Figures 2C–2D‴), indicating that Nub-PB and Nub-PD are also expressed in EBs. However, reporter lines are not optimal for following protein dynamics. Instead, immunostaining was used to analyze the cellular distribution of Nub, after first validating antibody specificity in nub^{E37} mutant clones (Figures S2B–S2B‴). Interestingly, we observed Nub immunostaining in the nucleus of cells expressing *esg-gal4* driven GFP (Figures 2E–2E‴) and *esg-lacZ*-positive cells (Figures 2F–2F‴), indicating that Nub protein is expressed in progenitor cells. However, not all progenitor cells stained with Nub antibody and staining was not uniform throughout the nucleus, suggesting a dynamic nature of Nub proteins and post-translational modifications. Interestingly, mammalian OCT1/POU2F1 display a dynamic behavior, with regulated sub-nuclear localization and post-translational modifications in response to cellular stress, which was suggested to correlate with changes in transcriptional activity (Boubriak et al., 2017; Kang et al., 2013; Malhas et al., 2009). To increase the number of progenitor cells we aimed at analyzing midguts undergoing frequent regeneration. For this, oral infections were performed with *Erwinia carotovora carotovora 15* (*Ecc15*) to induce ISC proliferation (Buchon et al., 2010). Importantly, the number of Nub-positive *esg-lacZ*-marked cells (Figures 2G–2G‴) increased upon *Ecc15* infection, validating that Nub is expressed in progenitor cells during stimulated regenerative conditions. To further analyze Nub expression in dividing cells, we analyzed *Drosophila malignant blood neoplasm-2 (mbn-2)* cells in culture. Interestingly, Nub immunostaining was observed specifically in cells during mitosis. Although weak Nub immunostaining was evident throughout the cytosol of the dividing cells, it was highly concentrated at the midbody during anaphase (Figure 2H″), overlapping with microtubuli, marked by β-tubulin immunostaining (Figures 2H and 2H‴). For additional confirmation, we analyzed Nub immunostaining in the Fly-specific fluorescent ubiquitination-based cell-cycle indicator cell line, which enables specific labeling of different cell phases during the cell cycle (Zielke et al., 2014). Cells in G1 and S phases are labeled by GFP and RFP, respectively, while cells in G2/M phases express both GFP and RFP and thus appear yellow (Figure S1D). Nub antibody-stained cells (Figure S1C‴) were expressing both GFP and RFP (Figures S1C–S1C‴) markers, demonstrating that Nub protein was present in these cells during the

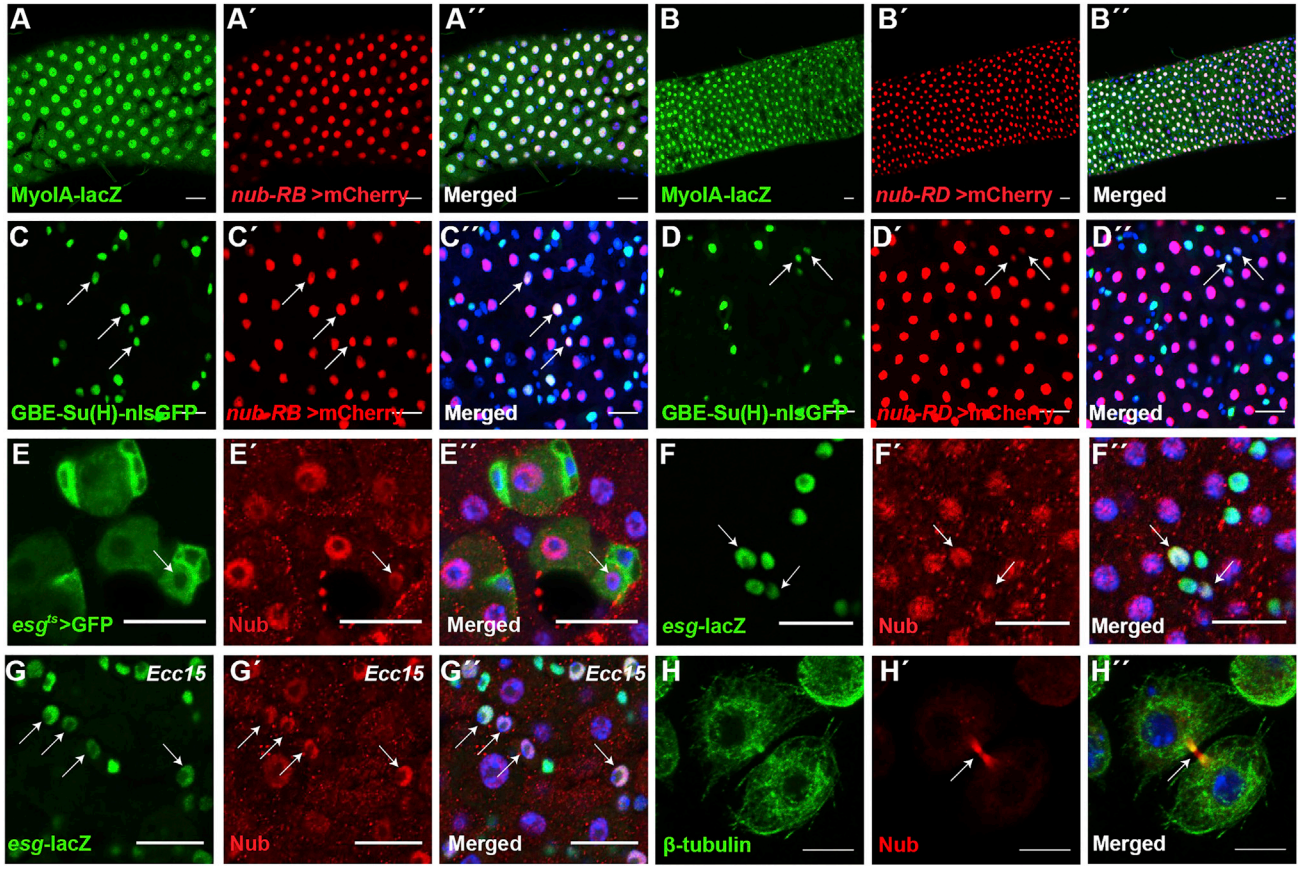

Figure 2. Localization of Nub in Adult Posterior Midgut and the mbn-2 Cell Line

(A–D″) Midguts expressing *nub-RB* > *mCherry* (A′–A″ and C′–C″; red) and *nub-RD* > *mCherry* (B′–B″ and D′–D″; red), combined with EC-specific reporter (A, A″ and B, B″; green) or an EB-specific Notch reporter (C, C″ and D, D″; green) in 5-day-old female posterior midguts. White arrows indicate cells positive for both GBE reporter (C–D″) and *nub-RB* reporter (C–C″) or *nub-RD* reporter (D–D″).

(E–F″) Nub antibody staining (E′, E″ and F′, F″; red) in 5-day-old female midguts with progenitor cells marked with esg^{ts} > *GFP* (E, E″; green) and *esg-lacZ* (F, F″; green). White arrows indicate cells positive for both Nub and *esg*-reporters.

(G–G″) Nub antibody staining (G′–G″; red) in 5-day-old *esg-lacZ* (green) female midguts upon *Ecc15* infection for 12 hr. Note the increased number of Nub/*esg*-positive cells (white arrows) after infection.

(H–H″) Immunostaining of *Drosophila* mbn-2 cells undergoing mitosis and cytokinesis using antibodies to Nub (H′–H″; red) and β-tubulin (H and H″; green). White arrows show Nub staining in the midbody structure during cytokinesis.

Scale bars, 20 μm in (A)–(G″) and 10 μm in (H)–(H″).

See also Figures S1 and S2.

G2/M phase. Taken together, antibody staining confirmed that Nub is expressed in actively dividing cells.

Loss of Nub-PB in Progenitor Cells Leads to Increased *esg* Expression and ISC Proliferation

Next, we aimed at characterizing the roles of the two Nub protein isoforms in the regulation of ISC activity and differentiation. While Nub-PD has been shown to confer proliferation in embryonic neuroblasts (Bahrampour et al., 2017), nothing is known about the function of Nub-PB. We used an RNAi line directed specifically against *nub-RB* in combination with the esg^{ts} *flip-out (F/O)* system (Jiang et al., 2009) to analyze whether Nub-PB is involved in turnover of posterior midgut epithelial cells. In midguts of control flies, *esg*-gal4 drives UAS-GFP expression in progenitor cells (ISC + EB) and, upon flip-out, small clusters of daughter cells were labeled by *actin*-gal4-driven GFP (Figure 3A). Overexpression of *nub-RB* for 7 days eliminated all GFP-marked cells (Figure 3B), indicating that no new progenitor cells were generated. In contrast, depletion of *nub-RB* promoted the growth of hyperplastic masses of GFP-positive cells (Figure 3C), indicating increased ISC proliferation and rapid epithelial turnover. To confirm this, we compared the number of mitotic cells by

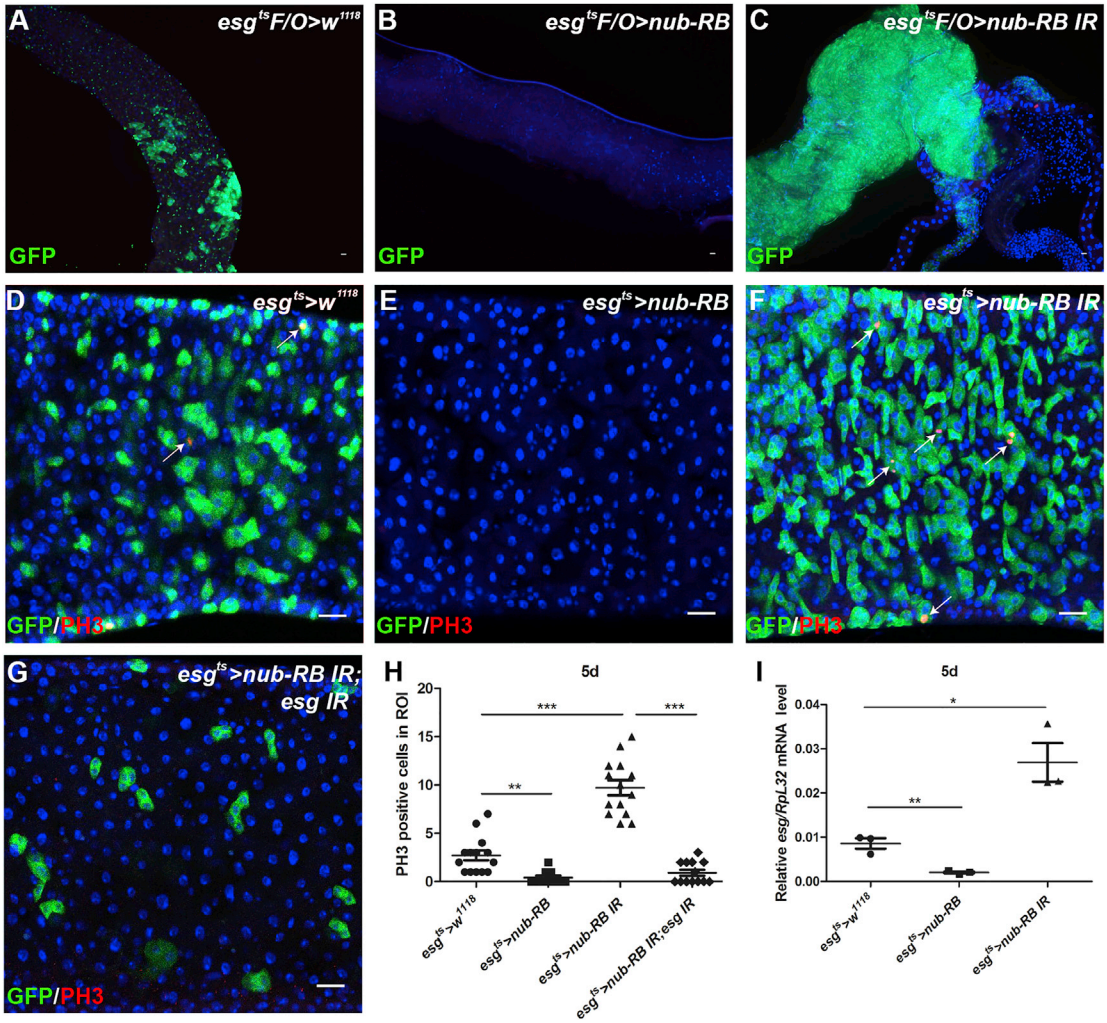

Figure 3. Nub-PB Regulates ISC Proliferation by Repression of *esg* Expression in Progenitor Cells

(A–C) Gut epithelial turnover experiments using *esg^{ts} F/O* system in posterior midguts, control (A), after *nub-RB* overexpression (B) and *nub-RB* downregulation (C) for 7 days, respectively.

(D–G) PH3 antibody staining (red) in 5-day-old control midguts (D), upon *nub-RB* overexpression (E), *nub-RB* downregulation (F), and co-downregulation of *nub-RB* and *esg* (G) in progenitor cells (ISC + EB, GFP-labeled) driven by *esg-gal4*. White arrows indicate PH3-positive cells. Scale bars, 20 μm in (A)–(G).

(H) Quantification of PH3-positive cells in the region of interest (ROI) (approximately R5 region; Buchon et al., 2013) from control (filled circles, n = 14), *nub-RB* overexpression (filled rectangles, n = 10), *nub-RB* downregulation (filled triangles, n = 14), and co-downregulation of *nub-RB* and *esg* (filled quadrangles, n = 13) midguts. Statistical significance was calculated using unpaired t test, $^{**}p < 0.01$, $^{***}p < 0.001$.

(I) Quantification of *esg* mRNA expression levels in guts dissected from control (filled circles, n = 3), *nub-RB* overexpression (filled rectangles, n = 3), and *nub-RB* downregulation (black triangles, n = 3) flies. Statistical significance was calculated using unpaired t test, $^{*}p < 0.05$, $^{**}p < 0.01$. Error bars in each graph represent SEM.

phospho-histone 3 (PH3) labeling following overexpression or downregulation of *nub-RB* in progenitor cells. The number of PH3-positive cells was significantly decreased upon *nub-RB* overexpression (Figures 3E and 3H) compared with control (Figures 3D and 3H). In contrast, *nub-RB* downregulation resulted in hyper-proliferation (Figures 3F and 3H). These results indicate that the role of Nub-PB is to block proliferation and to drive differentiation in the midgut. Recently, Esg has been reported to act as a stemness factor in adult midgut, as reducing *esg* expression in stem cells decreased their proliferative capacity (Korzelius et al., 2014). To examine whether *esg* is involved in *nub-RB* depletion-induced hyper-proliferation, we downregulated both *nub-RB* and *esg* in progenitor cells

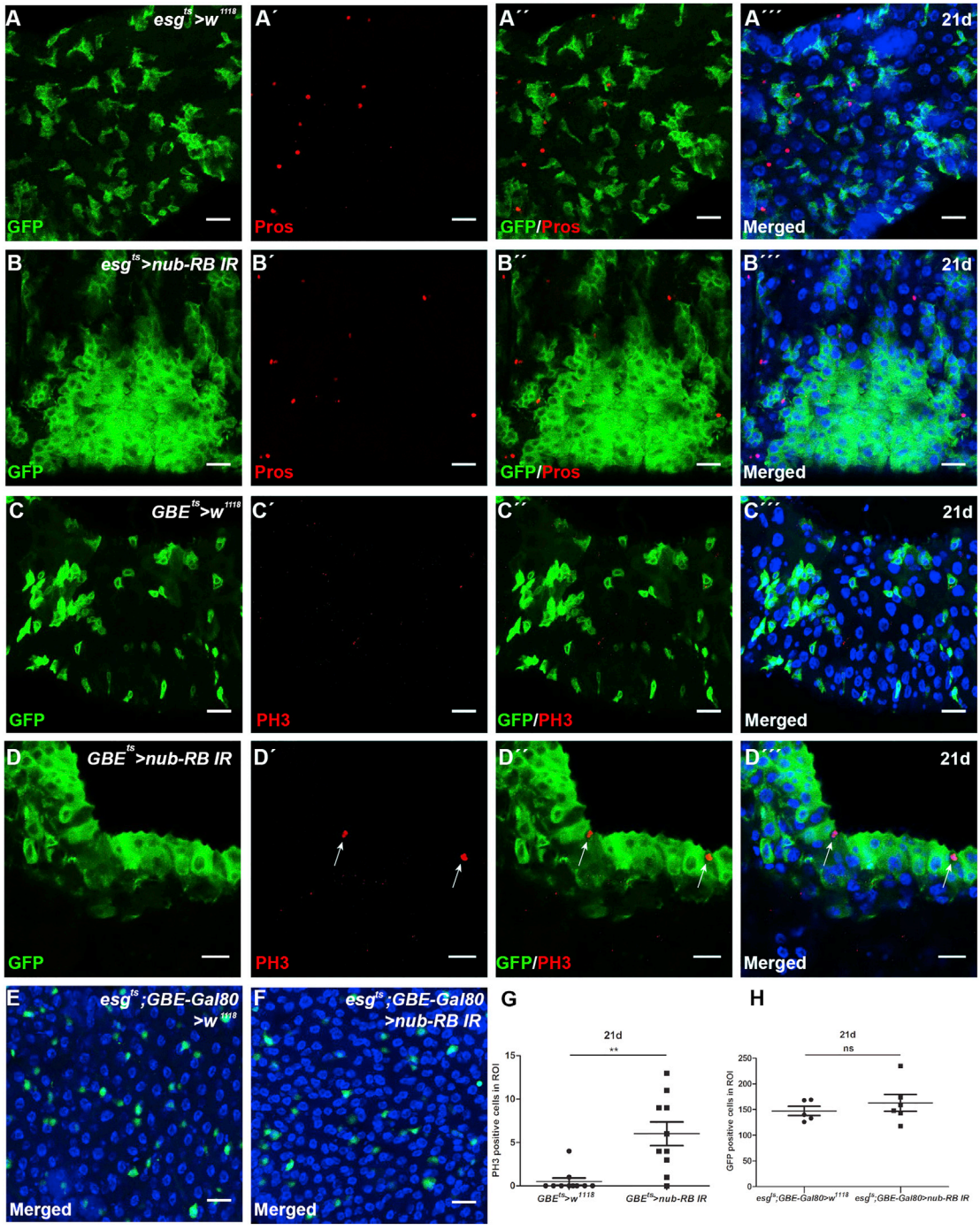

Figure 4. Nub-PB Functions in EBs to Control Differentiation

(A–B‴) Prospero (Pros) antibody staining (red) in the anterior midgut of control (A′–A‴) and after *nub-RB* downregulation (B′–B‴) in progenitor cells (ISC + EB, GFP-labeled) for 21 days.

(C–D‴) PH3 antibody staining (red) in the anterior midgut of control (C′–C‴), and after *nub-RB* downregulation (D′ and D‴) in EBs (GFP-labeled) for 21 days. Note that more mitotic cells are present upon *nub-RB* downregulation, white arrows in (D′–D‴).

(E and F) Downregulation of *nub-RB* specifically in ISCs (GFP-labeled) using *esg^{ts};GBE-Gal80* in anterior midgut for 21 days. Scale bars, 20 μm in (A)–(F).

(legend continued on next page)

and measured the rate of ISC proliferation. Importantly, this abolished the hyper-proliferative phenotype (Figures 3G and 3H), suggesting that *esg* is required for *nub-RB* depletion-induced ISC hyper-proliferation. In addition, *nub-RB* overexpression caused a significant decrease in *esg* expression (Figure 3I), whereas *nub-RB* downregulation promoted increased *esg* transcript levels (Figure 3I). This suggests that Nub-PB inhibits ISC proliferation in newly formed daughter cells, by direct or indirect repression of *esg* expression, promoting them to the exit the cell cycle and begin differentiation.

Nub-PB Functions in EBs to Regulate Differentiation

To clarify in which cell types Nub-PB normally acts to regulate proliferation and differentiation, we depleted *nub-RB* expression by RNAi either in ISCs (*esg^{ts};Su(H)GBE-Gal80*), in EBs (*Su(H)GBE-Gal80^{ts}*) (hereafter referred to *esg^{ts};GBE-Gal80* and *GBE^{ts}*, respectively), or in both (*esg^{ts}*). Reduction of *nub-RB* expression in ISC + EB cells with *esg-Gal4* for 21 days led to pronounced accumulation of non-differentiated *esg*-positive GFP clusters in the anterior and posterior midgut (Figures 4A–4B‴ and S3A–B″). This suggests that depletion of *nub-RB* in *esg*-positive cells is associated with loss of progenitor cell differentiation. This was confirmed by the absence of differentiated EE cells in the same region, using Prospero (Pros) antibody staining (Figures 4B–4B‴), indicating that both EC and EE lineage differentiation is defect. In the adult midgut, EBs are transient non-proliferative cells, which either differentiate rapidly after completing cell division and cytokinesis, or remain as EBs with the capacity to differentiate later (Micchelli and Perrimon, 2006; Ohlstein and Spradling, 2006). To investigate the role of Nub-PB in EBs, *nub-RB* was downregulated specifically in EBs by using *GBE^{ts}*. Strikingly, this also promoted strong accumulation of GFP-labeled cell clusters in the anterior and posterior midgut (Figures 4C–4D‴ and S3C–S3D″). Furthermore, there were more PH3-positive cells in the anterior midgut after *nub-RB* downregulation in EBs (Figures 4C″–4D‴ and 4G), suggesting that EB-specific *nub-RB* depletion increases ISC proliferation. In contrast, we did not observe any changes in cell proliferation or differentiation upon *nub-RB* downregulation in ISCs (Figures 4E, 4F, 4H, and S3E–S3F″), indicating that Nub-PB does not play a direct role in regulating stem cell activity. In summary, Nub-PB appears to specifically function in EBs to block proliferation and promote differentiation.

Overexpression of Nub-PB Rescues a Notch RNAi-Mediated Differentiation Defect

Notch signaling is a core pathway for controlling ISC fate specification and its inhibition leads to both ISC and EE tumor formation in the posterior midgut (Ohlstein and Spradling, 2007). As *nub-RB* RNAi in progenitor cells results in accumulation of non-differentiated progenitor-like cells, we next investigated whether Nub-PB is involved in Notch RNAi-mediated differentiation defects. As expected, downregulation of Notch in progenitor cells for 2 or 5 days resulted in both ISC and Pros-positive EE tumor formation (Figures 5A, 5B, 5E, and 5F), confirming that Notch signaling is required for both ISC proliferation and differentiation (Micchelli and Perrimon, 2006; Ohlstein and Spradling, 2007). Overexpression of *nub-RB* in progenitor cells for 2 days reduced the number of stem cells (Figure 5C) and erased almost all *esg*-positive GFP progenitor cells after 5 days (Figure 5G), approving that overexpression of *nub-RB* blocks stem cell proliferation (Figure 3). Importantly, downregulation of Notch did not cause ISC and EE tumor formation when combined with *nub-RB* overexpression for 2 or 5 days (Figures 5D and 5H), indicating that high expression levels of Nub-PB in progenitor cells rescues the Notch RNAi-mediated differentiation defect, including EE tumor formation. It has been shown that *esg* is required for Notch RNAi-induced tumor formation (Korzelius et al., 2014), and our data suggest that overexpression of *nub-RB* repressed *esg* expression (Figure 3). Taken together, these results show that Nub-PB acts as a tumor suppressor in Notch RNAi background, possibly by repression of *esg* expression, either directly or indirectly.

Nub-PD Is Required for Both Basal and Infection-Induced ISC Proliferation and Regulates ISC Fate in an Opposite Manner Compared with Nub-PB

To analyze the role of Nub-PD in regulation of ISC proliferation we measured the mitotic activity in midguts of the Nub-PD mutant *nub^{1}* by using PH3 antibody staining. The number of PH3-positive cells was significantly reduced in *nub^{1}* posterior midgut compared with control (Figures 6A–6C), indicating a low mitotic activity in Nub-PD mutant guts. Moreover, stem cell-specific Delta antibody staining confirmed reduced numbers of ISCs in *nub^{1}* midguts (Figures S4A–S4C). It was also evident that *nub^{1}* midguts display aberrant epithelium cell arrangements, with no or weak Armadillo staining (a cell adhesion marker) in

(G) Quantification of PH3-positive mitotic cells in the R2 region from control guts (C‴) (n = 10) and *nub-RB* downregulation guts (D‴) (n = 10).

(H) Quantification of GFP-labeled stem cell numbers in the R2 region in control guts (E) (n = 5) and after *nub-RB* downregulation (F) (n = 6). Statistical significance was calculated using unpaired t test, $^{**}p < 0.01$. ns, not significant. Error bars in each graph represent SEM. See also Figure S3.

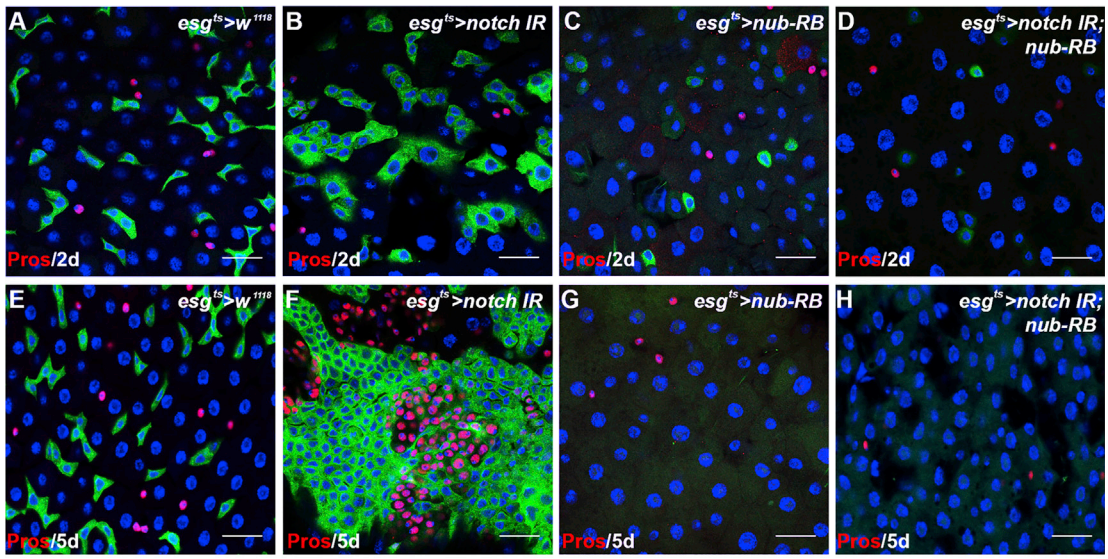

Figure 5. Overexpression of *nub-RB* Blocks Notch RNAi-Driven Differentiation Defects

Pros antibody staining (red) in 2-day-old (A–D) and 5-day-old (E–H) posterior midguts. Downregulation of *notch* in progenitor cells, driven by esg^{ts}, led to both ISC + EB (green) and EE (red) tumor-like cell formation (B and F) in posterior midguts compared with controls (A and E). *nub-RB* overexpression combined with *notch* IR in progenitor cells inhibits tumor formation both in 2-day-old (D) and 5-day-old (H) posterior midguts. Scale bars, 20 μm.

most ECs compared with control (Figures S4D and S4E), suggesting defects in the regeneration process. However, the EE lineage was not changed in nub^1 midguts, as the proportion of Pros-positive EE cells was comparable in control and nub^1 midguts (Figures S4D–S4F). Next, we investigated the mitotic activity in nub^1 midguts in response to *Ecc15* infection. As expected, fewer PH3-positive cells were found in nub^1 uninfected posterior midguts compared with controls (Figures 6D, 6F, and 6H), confirming the low level of ISC proliferative rate in nub^1 midguts. Importantly, *Ecc15* infection for 12 hr triggered ISC division both in control and nub^1 posterior midgut (Figures 6E, 6G, and H), but the number of $PH3^+$ cells in nub^1-infected midguts was significantly lower compared with infected control midguts (Figure 6H), suggesting that Nub-PD is required for full activation of ISC proliferation upon *Ecc15* infection. Taken together, Nub-PD is necessary for accurate rate of ISC proliferation both in basal and infection-induced conditions.

To investigate the interplay between Nub-PB and Nub-PD during cell fate determination we used MARCM system to track mitotic cell fates during development (Lee and Luo, 2001). MARCM was performed in Nub-PD mutant (nub^1) and Nub-PB/Nub-PD mutant (nub^{E37}) midguts to examine how Nub isoforms determine ISC fate. As shown in Figure 6, control clones (Figure 6I) became multicellular with an average number of 15–30 cells in each clone (Figure 6L), while nub^1 clones (Figure 6J) were always single-cell clones, confirming that Nub-PD is required for ISC proliferation. Strikingly, the nub^{E37}clones (Figure 6K), which lack both Nub-PD and Nub-PB, were multicellular and had similar cell numbers as the control (Figure 6L), indicating that, upon concomitant loss of both Nub-PB and Nub-PD, ISC proliferation is rescued. In addition, we observed many single-cell clones in the posterior midgut after overexpression of *nub-RB* both in controls (Figures S5B and S5J) and in nub^{E37} background (Figures S5E and S5J), suggesting that high levels of Nub-PB expression in progenitor cells indeed block ISC proliferation, which corroborates the results of Figure 3. Surprisingly, we did not observe any multicellular clones in the posterior midgut upon *nub-RD* overexpression in control background (Figures S5C and S5J) or in combination with the nub^{E37} background (Figures S5F and S5J), indicating that Nub-PD overexpression is not sufficient for activating ISC proliferation. Rather it blocked proliferation upon overexpression, a result that will be further discussed below.

The fact that the nub^{E37} MARCM clones resembled control clones with normal proliferation rate was surprising, and we decided to investigate this further with an independent approach, using a *nub-RB/RD IR* line, in which both *nub-RB* and *nub-RD* are targeted for degradation. In contrast to the hyper-proliferation caused by *nub-RB IR* (Figures S5G and S5H), expression of *nub-RB/RD IR* in progenitor cells rescued the hyper-proliferation (Figure S5I), demonstrating that the hyper-proliferation is Nub-PD dependent, and that

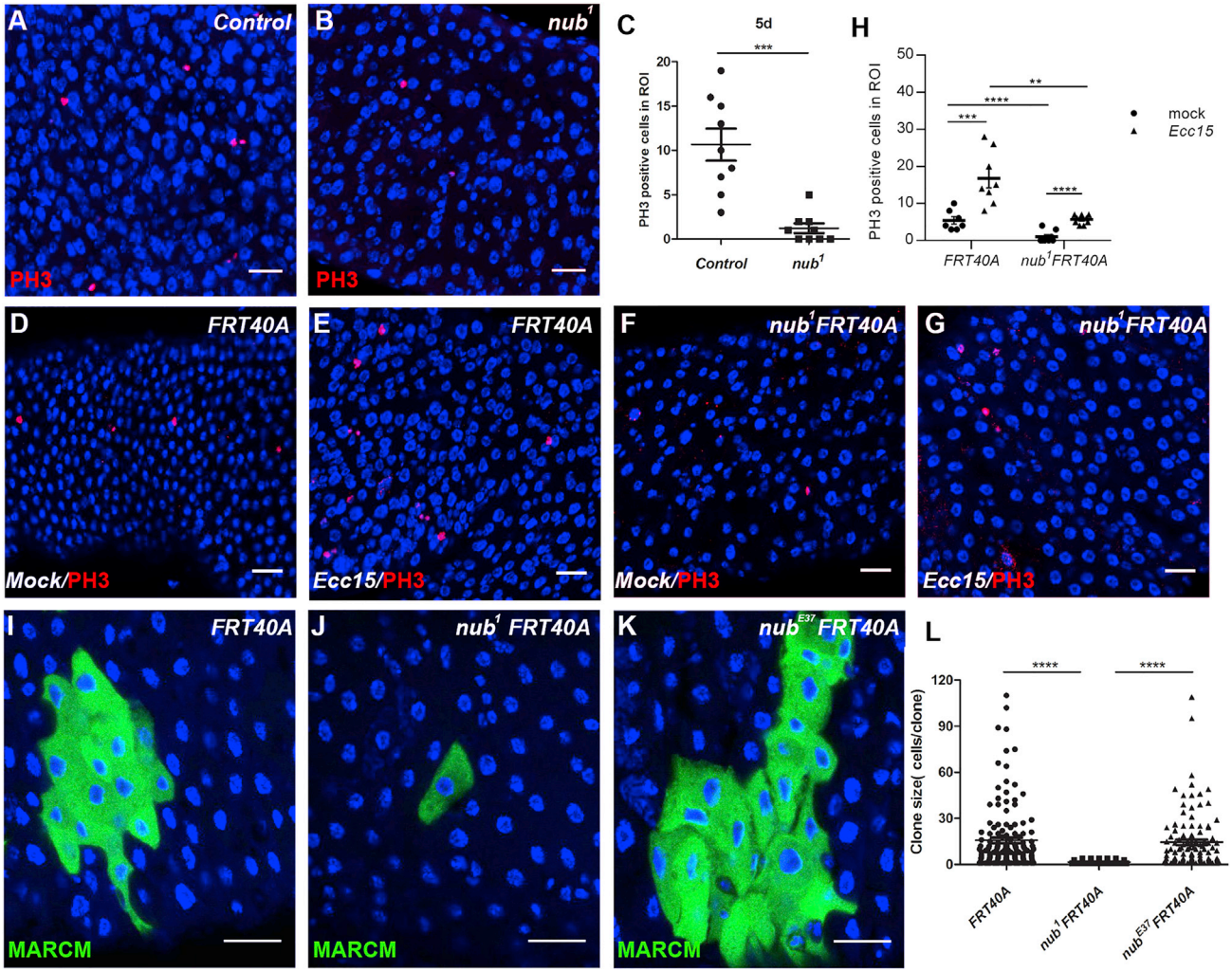

Figure 6. Nub-PD Is Required for Both Basal and Infection-Induced ISC Proliferation and Regulates ISC Proliferation in an Opposite Manner Compared with Nub-PB

(A and B) PH3 antibody staining (red) in 5-day-old control (A) and *nub*^{1} mutant (B).

(C) Quantification of PH3-positive cells in the R5 region from control guts (A) (n = 10) and *nub*^{1} mutant guts (B) (n = 10). Statistical significance was calculated using unpaired t test, ***p < 0.001.

(D–G) PH3 antibody staining (red) in 5-day-old control (*w+; FRT40A*) and *nub*^{1} mutant (*w+; nub*^{1}*FRT40A*) after mock (D and F) and *Ecc15* (E and G) infection for 12 hr.

(H) Quantification of PH3-positive cells in the R5 region, after *mock* and *Ecc15* infection (n = 7–9). Statistical significance was calculated using two-way ANOVA, Tukey's multiple comparisons test. **p < 0.01, ***p < 0.001, ****p < 0.0001.

(I–K) Lineage tracing analysis using MARCM system in control (I), *nub*^{1} (J), and *nub*^{E37} mutant (K) posterior midguts (R5 region).

(L) Quantification of the number of cells within each clone from control (I) (n = 142 clones), *nub*^{1} (J) (n = 91 clones), and *nub*^{E37} mutant (K) (n = 105 clones). Statistical significance was calculated using unpaired t test. ****p < 0.0001. Error bars in each graph represent SEM. Scale bars, 20 μm in (A), (B), (D)–(G), and (I)–(K). See also Figures S4 and S5.

concomitant loss of Nub-PB and Nub-PD restores cellular homeostasis. Thus, these results strongly indicate that Nub-PB and Nub-PD regulate ISC fate in opposite direction and suggest that the primary role of Nub-PD is to inhibit Nub-PB-driven differentiation, thereby ensuring ISC maintenance.

DISCUSSION

In the past few years, Nub/Pdm1 has been used as a marker of mature ECs in the *Drosophila* midgut (Beebe et al., 2010; Lee et al., 2009; Mathur et al., 2010), but a direct role in epithelium regeneration has not been fully investigated.

Here, we found that Nub isoforms are not only highly expressed in differentiated ECs, but also present in progenitor cells in the midgut. Nub immunostaining was not evident in all progenitor cells but specifically observed during mitosis and in a subset of EBs. This may either reflect that Nub protein concentration is very dynamic during the cell cycle or that antibodies directed against Nub are unable to detect its antigen during other phases of the cell cycle due to post-translational modifications and/or protein-protein interactions and complex formations. In addition to these immunostaining results, several global RNA sequence datasets of sorted midgut cells, such as the Flygut-seq (http://flygutseq.buchonlab.com/data) and (Zhai et al., 2015) have indicated expression of the *nub* gene in ISCs and EBs.

The observation that Nub immunostaining is enriched in the midbody of dividing cells may reflect a role of Nub either during the mitosis itself or directly after, in early G1 phase. In mammalian cells, OCT1/POU2F1 is phosphorylated in early mitosis and then concentrated in the midbody during cytokinesis, and was suggested to take part in regulation of mitosis (Kang et al., 2011). Importantly, both depletion and overexpression of OCT1/POU2F1 interfered with normal mitosis. Moreover, OCT4/POU5F1 is phosphorylated at the onset of mitosis and then dephosphorylated after exiting M phase. This cycle is necessary for its role in resetting the transcription machinery and to maintain ESC pluripotency (Shin et al., 2016). It is therefore plausible that the presence of OCT/POU proteins in mitotic cells, their post-translational modifications, and their role as transcriptional regulators in early G1 phase is important for regulation of normal stem cell division and for re-entering another round of the cell cycle.

Mammalian Oct/Pou genes are also producing several isoforms, but knowledge about their specific roles is relatively limited (Zhao, 2013). However, it was recently reported that different isoforms made from the human Oct1/Pou2f1 gene control expression of distinct sets of genes (Pankratova et al., 2016). Interestingly, these OCT1 isoforms are produced from transcripts initiated at independent transcriptional start sites, giving rise to three OCT1 isoforms with different N termini but identical DNA-binding domains, resembling how the *nub* gene is organized. The genes for Oct2/Pou2f1 and Oct4/Pou2f11 also produce several isoforms via alternative splicing. These different isoforms have been suggested to regulate neural differentiation, pluripotency, and some have been linked to malignancy (Zhao, 2013).

Here, we show that *Drosophila* Nub isoforms are involved both in the maintenance of the stemness of ISCs and in the differentiation of the EB to EC lineage. The role of Nub-PD as a stemness factor was demonstrated by the loss of ISC proliferation in whole midguts and in MARCM clones (Figure 6). However, overexpression of *nub-RD* did not activate cell division in the MARCM clones (Figure S5), but rather promoted differentiation. This result corroborates the findings of Korzelius et al., (2014), who reported that overexpression of Nub-PD in gut progenitor cells forced differentiation into ECs. One possibility is that the concentration of Nub-PD in ISCs is critical, and that overloading the cell with Nub-PD causes cell-cycle exit and differentiation. Importantly, the dosage of OCT4 is critical for maintaining stem cell self-renewal of ESCs, and both up- and downregulation of OCT4 induce differentiation into alternative lineages (Niwa et al., 2000). Similarly, accurate concentration of OCT1 was critical for normal mitotic progression (Kang et al., 2011). In the *Drosophila* embryonic nervous system, misexpression of Nub-PD results in neuroblast proliferation (Bahrampour et al., 2017; Bhat and Apsel, 2004; Bhat et al., 1995). It is therefore evident that Nub-PD has the capacity to stimulate neurogenic stem cells to proliferate.

A recent paper reported that one of the Snail family transcription factors, Esg, could directly bind to the promoter region of the *nub* gene and repress its expression, and it was suggested that such repression is necessary to maintain ISC identity (Korzelius et al., 2014). However, the study did not consider the two isoforms encoded by the *nub* gene and only focused on Nub-PD. Furthermore, it was suggested that Esg and Nub might have bidirectional regulatory roles in progenitor cells in different conditions (Korzelius et al., 2014). Here we show that overexpression of *nub-RB* in progenitor cells blocks ISC proliferation, possibly by downregulation of *esg* expression, either directly or indirectly. In correlation with this, downregulation of *nub-RB* by RNAi in progenitor cells elevated the expression level of *esg* and activation of ISC proliferation (Figure 3). Moreover, the hyper-proliferation phenotype induced by *nub-RB* RNAi was abolished when *esg* was depleted simultaneously. It is therefore likely that Nub-PB is controlling *esg* expression in progenitor cells, thereby prohibiting ISC proliferation. Moreover, *nub-RB* RNAi results indicate that Nub-PB is normally repressing proliferation in EBs. As a consequence, the increase in PH3 labeling upon EB-specific *nub-RB* RNAi is most likely a result of both ISC daughter cells maintaining self-renewal capacity in the absence of Nub-PB and sustained *esg* expression.

We propose a model for of how Nub-PB and Nub-PD may regulate ISC proliferation and differentiation (Figure 7). In this model, Nub-PB acts as a repressor of *esg* expression in progenitor cells, promoting differentiation of one of the daughter cells to an EB. Nub-PD, which counteracts the activity of Nub-PB, will thereby inhibit differentiation and allow stem cells to continue to divide, i.e., to maintain stemness. In the absence of Nub-PD (nub^1 mutant clones),

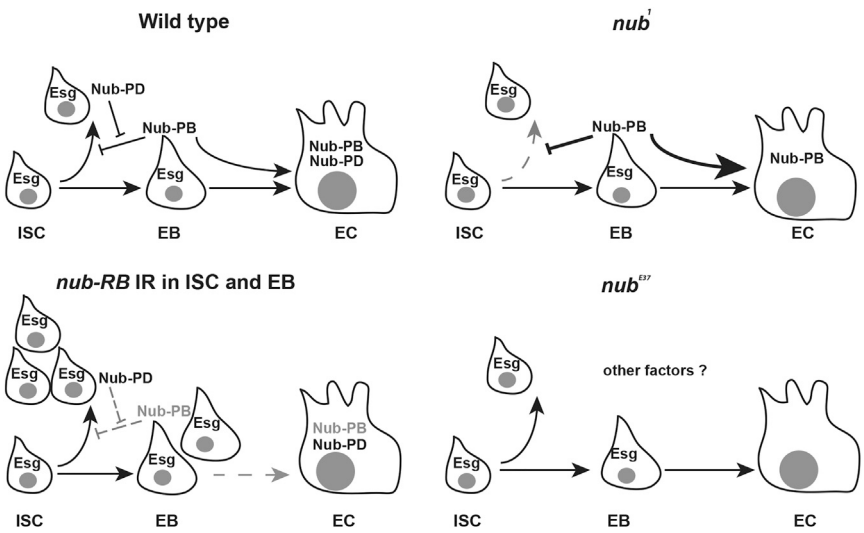

Figure 7. Proposed Model for *nub* Gene Regulation of ISC Proliferation and Differentiation

In wild-type condition, Nub-PB and Nub-PD are highly expressed in differentiated ECs. In addition, Nub-PB and Nub-PD are transiently expressed in progenitor cells. The present results indicate that Nub-PB specifically functions in EBs to block ISC proliferation and to promote differentiation toward EC fate. The mechanism for Nub-PB-driven proliferation inhibition is suggested to involve repression of Esg function, which is required for ISC proliferation. In the proposed model, Nub-PB activity is repressed by Nub-PD, allowing *esg* expression, stem cell maintenance and division. In nub^{1} mutants, ISC proliferation is, however, severely compromised due to the loss of Nub-PD, and therefore Nub-PB will drive rapid EB differentiation to Nub-PB-positive ECs. In contrast, downregulation of *nub-RB* in progenitor cells will trigger ISC proliferation by increasing the expression level of *esg*, and the loss of Nub-PB will also inhibit differentiation of EBs to ECs. In nub^{E37} mutant clones, ISCs display normal proliferation and differentiation rate possibly due to compensation by other unknown factors. Filled gray circles indicate nuclei and dashed gray lines or text indicate weak activity or expression.

Nub-PB will push both daughter cells to exit the cell cycle and promote rapid differentiation, hence, the stem cells will be lost and no more cell divisions will occur. In contrast, depletion of Nub-PB (*nub-RB* IR) will lead to a continuously high level of *esg* expression and enable both daughter cells to continue to divide, promoting increased number of ISCs. In this model, the primary role of Nub-PD is to repress the activity of Nub-PB on its target genes, meaning that midguts lacking both Nub-PB and Nub-PD would have a relatively normal cell cycle and rate of proliferation, which was the case in the nub^{E37} null mutant, as well as upon *nub-RB/RD* RNAi in progenitor cells. This may imply that the *nub* gene itself is dispensable for ISC proliferation during basal conditions. However, the *Drosophila pdm2* gene, which is a *nub* paralog, has been shown to confer a redundant role during neuroblast cell proliferation and specification in the embryo (Bhat et al., 1995). It is, therefore, possible that Pdm2 can compensate for the loss of *nub* and maintain normal ISC proliferation rate. In contrast, unbalanced expression of the two Nub protein isoforms, either as a result of overexpression or RNAi, interfered with cell proliferation in all variants tested. Thus, well-tuned expression of the two Nub protein isoforms is necessary for normal ISC proliferation and differentiation. Moreover, it was recently reported that Nub-PB and Nub-PD regulate the expression of immune genes in gut ECs in an antagonistic manner (Lindberg et al., 2018), pointing to the possibility that Nub-PB and Nub-PD play important roles in controlling epithelial renewal in the gut upon infection. This is supported by the fact that in nub^{1} mutants, ISC proliferation was considerably reduced (Figures 6A–6H), suggesting that Nub-PD is also required for infection-induced stem cell division.

In a recent study, Shen et al. (2017) found that mammalian POU2F1/OCT1 and POU5F1/OCT4 occupy both overlapping and independent sets of target genes in ESCs and their daughters. Importantly, concomitant with the loss of OCT4 binding, OCT1 occupancy increased during differentiation (Shen et al., 2017). This implies that POU/OCT factors may act in succession to regulate developmental processes based on sequential binding to common targets. Phylogenetic analyses have indicated that *Drosophila* and other invertebrates lack POU5 factors, i.e., direct homologs of OCT4/POU5F1, while Nub is most closely related to mammalian OCT1/POUF1 and OCT2/POUF2 (Gold et al., 2014). Importantly, though, it was shown using high-throughput SELEX experiments that the DNA binding specificity is highly conserved between mouse/human OCT4, OCT1, and *Drosophila* Nub (Nitta et al., 2015). This suggests that Nub proteins are in fact functionally related to both OCT4 and OCT1 in terms of DNA binding specificity. We speculate that Nub-PD shares functional analogy with OCT4 and OCT1 in sustaining stem cell renewal capacity, and thereby also restoring multipotency (OCT4 and Nub-PD), and that Nub-PB acts analogous to OCT1 in supporting differentiation of specific cell lineages. It is well established that mammalian POU/OCT factors act as crucial regulators of stemness, multipotency, and

differentiation. This work suggests that these properties of POU/OCT factors are evolutionarily ancient, operating in organisms as divergent as *Drosophila* and mammals.

EXPERIMENTAL PROCEDURES

Immunofluorescence Staining and Imaging

All crosses were set up at 18°C, then F1 progenies were kept at 18°C for 3–7 days before transferring to 29°C for initiation of GAL4 activity. Otherwise, flies were reared at 25°C.

Female intestines were dissected in PBS, pH 7.4 (PBS) and fixed in 4% paraformaldehyde for 1 hr at room temperature (RT), then briefly washed in PBST (PBS with 0.1% Triton X-100) and blocked with PBST+ 0.5% normal goat serum for 30 min at RT. The tissues were incubated with primary antibodies at 4°C overnight on a shaker. Next day, samples were washed in PBST (4 × 15 min) and incubated with secondary antibodies at RT for 2 hr on a shaker. Finally, samples were mounted in DABCO (Sigma) on a glass slide after staining with DAPI (Sigma). Images were taken by LSM 780 (Zeiss) or LSM 500 (Zeiss) and processed with Adobe Photoshop CS6 and Adobe Illustrator CS6.

RT-qPCR

Total RNA was extracted from 20 to 30 adult females' intestines with TRIzol (Bioline). cDNA synthesis and PCR were done as described previously (Dantoft et al., 2013). TaqMan Gene Expression Assays (Applied Biosystems) were used to quantify the given gene expression (TaqMan probes: *esg*: Dm01841264_s1; Applied Biosystems); all experiments were analyzed in biological triplicates and the measured mRNA expression level were normalized relative to those of *RpL32*.

Statistical Analysis

Statistical significances were calculated using either unpaired t test in pairwise comparisons or one- or two-way ANOVA combined with Tukey's *post hoc* test in multiple comparisons as shown in related figures. Graphical plotting was done in GraphPad Prism 6.0.

SUPPLEMENTAL INFORMATION

Supplemental Information includes Supplemental Experimental Procedures and five figures and can be found with this article online at https://doi.org/10.1016/j.stemcr.2018.03.014.

AUTHOR CONTRIBUTIONS

Conceptualization, X.T., Y.Z., B.N., and Y.E.; Methodology and Investigation, X.T., Y.Z., B.N., and Y.E.; Data Analysis, X.T. and Y.Z.; Writing – Original Draft, X.T. and Y.E. with input from all authors; Writing – Review & Editing, X.T., Y.Z., B.N., and Y.E.; Funding Acquisition, Y.E.

ACKNOWLEDGMENTS

We want to express our thanks to Bloomington *Drosophila* Stock Center and Vienna *Drosophila* RNAi Center for fly stocks, the Developmental Studies Hybridoma Bank for antibodies, the *Drosophila* Genomics Resource Center for cDNA clones, Heinrich Reichert, Wes Gruber, and Tetsuya Kojima for *FRT40A*, *nub*^{1} *FRT40A*, and *nub*^{E37} *FRT40A* flies, Ulrich Theopold and Spyros Artavanis-Tsakonas for *UAS-Notch IR* flies, Joaquin de Navascués for *GBE-Su[H]-nlsGFP* flies, Bruno Lemaitre for *Ecc15* bacterial strain, Bill Chia and Yu Cai for Nub antibody, and the Imaging Facility at Stockholm University for technical support. We are grateful to Bo Lindberg for invaluable discussions and for critically reviewing the manuscript. The authors declare that they have no conflict of interest.

Received: December 6, 2017
Revised: March 19, 2018
Accepted: March 20, 2018
Published: April 19, 2018

REFERENCES

Amcheslavsky, A., Jiang, J., and Ip, Y.T. (2009). Tissue damage-induced intestinal stem cell division in *Drosophila*. Cell Stem Cell *4*, 49–61.

Apidianakis, Y., and Rahme, L.G. (2011). *Drosophila* melanogaster as a model for human intestinal infection and pathology. Dis. Model Mech. *4*, 21–30.

Bahrampour, S., Gunnar, E., Jonsson, C., Ekman, H., and Thor, S. (2017). Neural lineage progression controlled by a temporal proliferation program. Dev. Cell *43*, 332–348.e4.

Bardin, A.J., Perdigoto, C.N., Southall, T.D., Brand, A.H., and Schweisguth, F. (2010). Transcriptional control of stem cell maintenance in the *Drosophila* intestine. Development *137*, 705–714.

Barker, N., van de Wetering, M., and Clevers, H. (2008). The intestinal stem cell. Genes Dev. *22*, 1856–1864.

Beebe, K., Lee, W.C., and Micchelli, C.A. (2010). JAK/STAT signaling coordinates stem cell proliferation and multilineage differentiation in the *Drosophila* intestinal stem cell lineage. Dev. Biol. *338*, 28–37.

Bergman, P., Seyedoleslami Esfahani, S., and Engström, Y. (2017). *Drosophila* as a model for human diseases-focus on innate immunity in barrier epithelia. Curr. Top. Dev. Biol. *121*, 29–81.

Bhat, K.M., and Apsel, N. (2004). Upregulation of Mitimere and Nubbin acts through Cyclin E to confer self-renewing asymmetric division potential to neural precursor cells. Development *131*, 1123–1134.

Bhat, K.M., Poole, S.J., and Schedl, P. (1995). The miti-mere and Pdm1 genes collaborate during specification of the Rp2/Sib lineage in *Drosophila* neurogenesis. Mol. Cell Biol. *15*, 4052–4063.

Biteau, B., Hochmuth, C.E., and Jasper, H. (2008). JNK activity in somatic stem cells causes loss of tissue homeostasis in the aging *Drosophila* gut. Cell Stem Cell *3*, 442–455.

Biteau, B., and Jasper, H. (2014). Slit/robo signaling regulates cell fate decisions in the intestinal stem cell lineage of *Drosophila*. Cell Rep. *7*, 1867–1875.

Boubriak, I.I., Malhas, A.N., Drozdz, M.M., Pytowski, L., and Vaux, D.J. (2017). Stress-induced release of Oct-1 from the nuclear envelope is mediated by JNK phosphorylation of lamin B1. PLoS One *12*, e0177990.

Buchon, N., Broderick, N.A., Kuraishi, T., and Lemaitre, B. (2010). *Drosophila* EGFR pathway coordinates stem cell proliferation and gut remodeling following infection. BMC Biol. *8*, 152.

Buchon, N., Broderick, N.A., Poidevin, M., Pradervand, S., and Lemaitre, B. (2009). *Drosophila* intestinal response to bacterial infection: activation of host defense and stem cell proliferation. Cell Host Microbe *5*, 200–211.

Buchon, N., Osman, D., David, F.P.A., Fang, H.Y., Boquete, J.P., Deplancke, B., and Lemaitre, B. (2013). Morphological and molecular characterization of adult midgut compartmentalization in *Drosophila*. Cell Rep. *3*, 1725–1738.

Dantoft, W., Davis, M.M., Lindvall, J.M., Tang, X.Z., Uvell, H., Junell, A., Beskow, A., and Engstrom, Y. (2013). The Oct1 homolog Nubbin is a repressor of NF-kappa B-dependent immune gene expression that increases the tolerance to gut microbiota. BMC Biol. *11*, 99.

Dantoft, W., Lundin, D., Esfahani, S.S., and Engstrom, Y. (2016). The POU/Oct transcription factor Pdm1/nub is necessary for a beneficial gut microbiota and normal lifespan of *Drosophila*. J. Innate Immun. *8*, 412–426.

Dutta, D., Dobson, A.J., Houtz, P.L., Glasser, C., Revah, J., Korzelius, J., Patel, P.H., Edgar, B.A., and Buchon, N. (2015). Regional cell-specific transcriptome mapping reveals regulatory complexity in the adult *Drosophila* midgut. Cell Rep. *12*, 346–358.

Gold, D.A., Gates, R.D., and Jacobs, D.K. (2014). The early expansion and evolutionary dynamics of POU class genes. Mol. Biol. Evol. *31*, 3136–3147.

Guo, Z., and Ohlstein, B. (2015). Stem cell regulation. Bidirectional Notch signaling regulates *Drosophila* intestinal stem cell multipotency. Science *350*. https://doi.org/10.1126/science.aab0988.

Holland, P.W.H., Booth, H.A.F., and Bruford, E.A. (2007). Classification and nomenclature of all human homeobox genes. BMC Biol. *5*, 47.

Jiang, H.Q., Patel, P.H., Kohlmaier, A., Grenley, M.O., McEwen, D.G., and Edgar, B.A. (2009). Cytokine/Jak/Stat signaling mediates regeneration and homeostasis in the *Drosophila* midgut. Cell *137*, 1343–1355.

Kang, J., Goodman, B., Zheng, Y.X., and Tantin, D. (2011). Dynamic regulation of Oct1 during mitosis by phosphorylation and ubiquitination. PLoS One *6*, e23872.

Kang, J., Shen, Z.L., Lim, J.M., Handa, H., Wells, L., and Tantin, D. (2013). Regulation of Oct1/Pou2f1 transcription activity by O-GlcNAcylation. FASEB J. *27*, 2807–2817.

Korzelius, J., Naumann, S.K., Loza-Coll, M.A., Chan, J.S., Dutta, D., Oberheim, J., Glasser, C., Southall, T.D., Brand, A.H., Jones, D.L., et al. (2014). Escargot maintains stemness and suppresses differentiation in *Drosophila* intestinal stem cells. EMBO J. *33*, 2967–2982.

Kvon, E.Z., Kazmar, T., Stampfel, G., Yanez-Cuna, J.O., Pagani, M., Schernhuber, K., Dickson, B.J., and Stark, A. (2014). Genome-scale functional characterization of *Drosophila* developmental enhancers in vivo. Nature *512*, 91–95.

Lee, T.M., and Luo, L.Q. (2001). Mosaic analysis with a repressible cell marker (MARCM) for *Drosophila* neural development. Trends Neurosci. *24*, 251–254.

Lee, W.C., Beebe, K., Sudmeier, L., and Micchelli, C.A. (2009). Adenomatous polyposis coli regulates *Drosophila* intestinal stem cell proliferation. Development *136*, 2255–2264.

Li, H.J., and Jasper, H. (2016). Gastrointestinal stem cells in health and disease: from flies to humans. Dis. Model Mech. *9*, 487–499.

Lindberg, B.G., Tang, X., Dantoft, W., Gohel, P., Seyedoleslami Esfahani, S., Lindvall, J.M., and Engström, Y. (2018). Nubbin isoform antagonism governs *Drosophila* intestinal immune homeostasis. PLoS Pathog. *14*, e1006936.

Liu, X., Hodgson, J.J., and Buchon, N. (2017). *Drosophila* as a model for homeostatic, antibacterial, and antiviral mechanisms in the gut. PLoS Pathog. *13*, e1006277.

Malhas, A.N., Lee, C.F., and Vaux, D.J. (2009). Lamin B1 controls oxidative stress responses via Oct-1. J. Cell. Biol. *184*, 45–55.

Mathur, D., Bost, A., Driver, I., and Ohlstein, B. (2010). A transient niche regulates the specification of *Drosophila* intestinal stem cells. Science *327*, 210–213.

Micchelli, C.A. (2012). The origin of intestinal stem cells in *Drosophila*. Dev. Dyn. *241*, 85–91.

Micchelli, C.A., and Perrimon, N. (2006). Evidence that stem cells reside in the adult *Drosophila* midgut epithelium. Nature *439*, 475–479.

Ng, M., Diazbenjumea, F.J., and Cohen, S.M. (1995). Nubbin encodes a Pou-domain protein required for proximal-distal patterning in the *Drosophila* wing. Development *121*, 589–599.

Nitta, K.R., Jolma, A., Yin, Y.M., Morgunova, E., Kivioja, T., Akhtar, J., Hens, K., Toivonen, J., Deplancke, B., Furlong, E.E.M., et al. (2015). Conservation of transcription factor binding specificities across 600 million years of bilateria evolution. eLife *4*.

Niwa, H., Miyazaki, J., and Smith, A.G. (2000). Quantitative expression of Oct-3/4 defines differentiation, dedifferentiation or self-renewal of ES cells. Nat. Genet. *24*, 372–376.

Ohlstein, B., and Spradling, A. (2006). The adult *Drosophila* posterior midgut is maintained by pluripotent stem cells. Nature *439*, 470–474.

Ohlstein, B., and Spradling, A. (2007). Multipotent *Drosophila* intestinal stem cells specify daughter cell fates by differential Notch signaling. Science *315*, 988–992.

Pankratova, E.V., Stepchenko, A.G., Portseva, T., Mogila, V.A., and Georgieva, S.G. (2016). Different N-terminal isoforms of Oct-1 control expression of distinct sets of genes and their high levels in Namalwa Burkitt's lymphoma cells affect a wide range of cellular processes. Nucleic Acids Res. *44*, 9218–9230.

Patel, P.H., Dutta, D., and Edgar, B.A. (2015). Niche appropriation by *Drosophila* intestinal stem cell tumours. Nat. Cell Biol. *17*, 1182–1192.

Perdigoto, C.N., Schweisguth, F., and Bardin, A.J. (2011). Distinct levels of Notch activity for commitment and terminal differentiation of stem cells in the adult fly intestine. Development *138*, 4585–4595.

Ren, F.F., Wang, B., Yue, T., Yun, E.Y., Ip, Y.T., and Jiang, J. (2010). Hippo signaling regulates *Drosophila* intestine stem cell proliferation through multiple pathways. Proc. Natl. Acad. Sci. USA *107*, 21064–21069.

Shen, Z.L., Kang, J.S., Shakya, A., Tabaka, M., Jarboe, E.A., Regev, A., and Dean, T.T. (2017). Enforcement of developmental lineage specificity by transcription factor Oct1. eLife *6*.

Shin, J., Kim, T.W., Kim, H., Kim, H.J., Suh, M.Y., Lee, S., Lee, H.T., Kwak, S., Lee, S.E., Lee, J.H., et al. (2016). Aurkb/PP1 mediated resetting of Oct4 during the cell cycle determines the identity of embryonic stem cells. eLife *5*, e10877.

Takahashi, K., and Yamanaka, S. (2006). Induction of pluripotent stem cells from mouse embryonic and adult fibroblast cultures by defined factors. Cell *126*, 663–676.

Tantin, D. (2013). Oct transcription factors in development and stem cells: insights and mechanisms. Development *140*, 2857–2866.

Tian, A.G., and Jiang, J. (2014). Intestinal epithelium-derived BMP controls stem cell self-renewal in *Drosophila* adult midgut. eLife *3*, e018457.

Venken, K.J.T., Schulze, K.L., Haelterman, N.A., Pan, H.L., He, Y.C., Evans-Holm, M., Carlson, J.W., Levis, R.W., Spradling, A.C., Hoskins, R.A., et al. (2011). MiMIC: a highly versatile transposon insertion resource for engineering *Drosophila* melanogaster genes. Nat. Methods *8*, 737–743.

Yeo, S.L., Lloyd, A., Kozak, K., Dinh, A., Dick, T., Yang, X.H., Sakonju, R., and Chia, W. (1995). On the functional overlap between 2 *Drosophila* Pou homeo domain genes and the cell fate specification of a CNS neural precursor. Genes Dev. *9*, 1223–1236.

Zeng, X.K., and Hou, S.X. (2015). Enteroendocrine cells are generated from stem cells through a distinct progenitor in the adult *Drosophila* posterior midgut. Development *142*, 644–653.

Zhai, Z., Kondo, S., Ha, N., Boquete, J.P., Brunner, M., Ueda, R., and Lemaitre, B. (2015). Accumulation of differentiating intestinal stem cell progenies drives tumorigenesis. Nat. Commun. *6*, 10219.

Zhao, F.Q. (2013). Octamer-binding transcription factors: genomics and functions. Front Biosci. (Landmark Ed.) *18*, 1051–1071.

Zielke, N., Korzelius, J., van Straaten, M., Bender, K., Schuhknecht, G.F.P., Dutta, D., Xiang, J.Y., and Edgar, B.A. (2014). Fly-FUCCI: a versatile tool for studying cell proliferation in complex tissues. Cell Rep. *7*, 588–598.

Stem Cell Reports, Volume *10*

Supplemental Information

The POU/Oct Transcription Factor Nubbin Controls the Balance of Intestinal Stem Cell Maintenance and Differentiation by Isoform-Specific Regulation

Xiongzhuo Tang, Yunpo Zhao, Nicolas Buchon, and Ylva Engström

1. Supplemental Figures and Legends

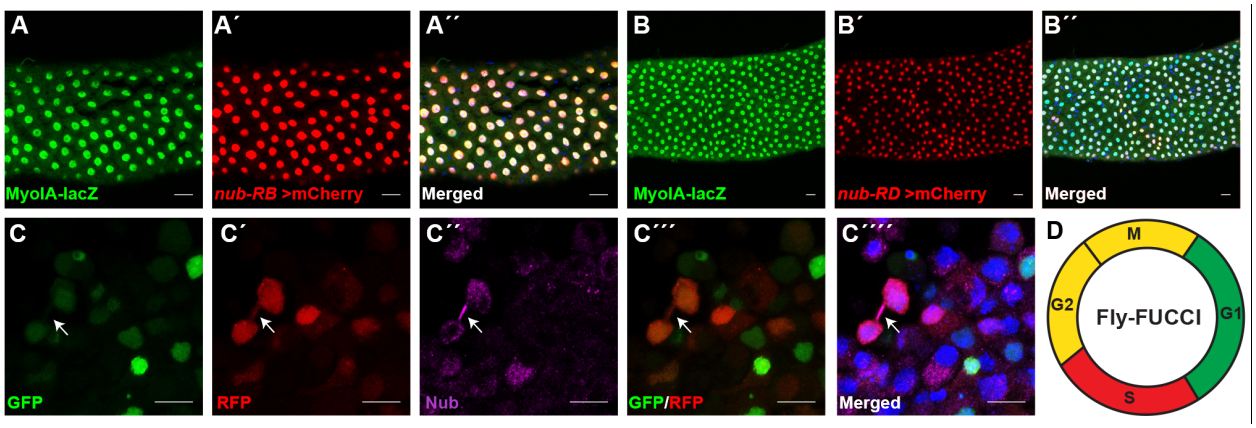

Figure S1. Expression pattern of Nub in adult anterior midgut and Fly FUCCI cell line. Related to Figure 2.

A-B´´: Expression of *nub-RB* and *nub-RD* specific Gal4 lines driving mCherry (red), overlapping with *MyolA-LacZ* (green) expression in the anterior midgut. A´´ and B´´ are merged pictures. **´C-C´´´´:** Nub antibody staining (magenta in C´´) in the Fly FUCCI cell line. Cells in G1 phase are labeled by GFP (green in C), S phase cells are labeled by RFP (red in C´), G2/M phase appears yellow (C´´´). Nuclei are labeled with DAPI (blue, C´´´´). White arrows indicate cells positive for Nub expression during G2/M phase. **D:** Color code for the Fly FUCCI cell labeling. Scale bars in A-B´´ represent 20 µm; Scale bars in C-C´´´´ represent 10 µm.

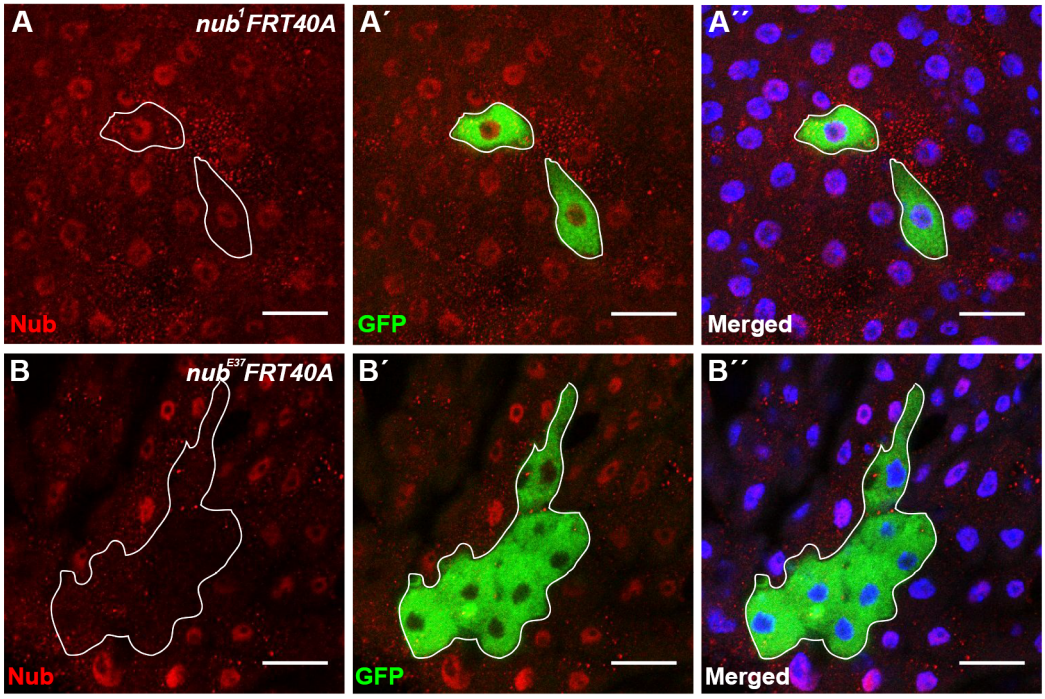

Figure S2. Nub protein is expressed in *nub^{1}FRT40A* clones, but not in *nub^{E37}FRT40A* clone. Related to Figure 2**.**

A-B´´: Verification of Nub antibody specificity in *nub* mutant clones. Nub antibody staining (red) in *nub^{1}FRT40A* clones (A´) and in *nub^{E37}FRT40A* clone (B´). A´´ and B´´ are merged pictures. Note that Nub antibody staining is missing in *nub^{E37}FRT40A* clone, but present in *nub^{1}FRT40A* clones, which lacks the Nub-PD protein but expresses Nub-PB. White lines indicate clone borders. Scale bars represent 20 µm.

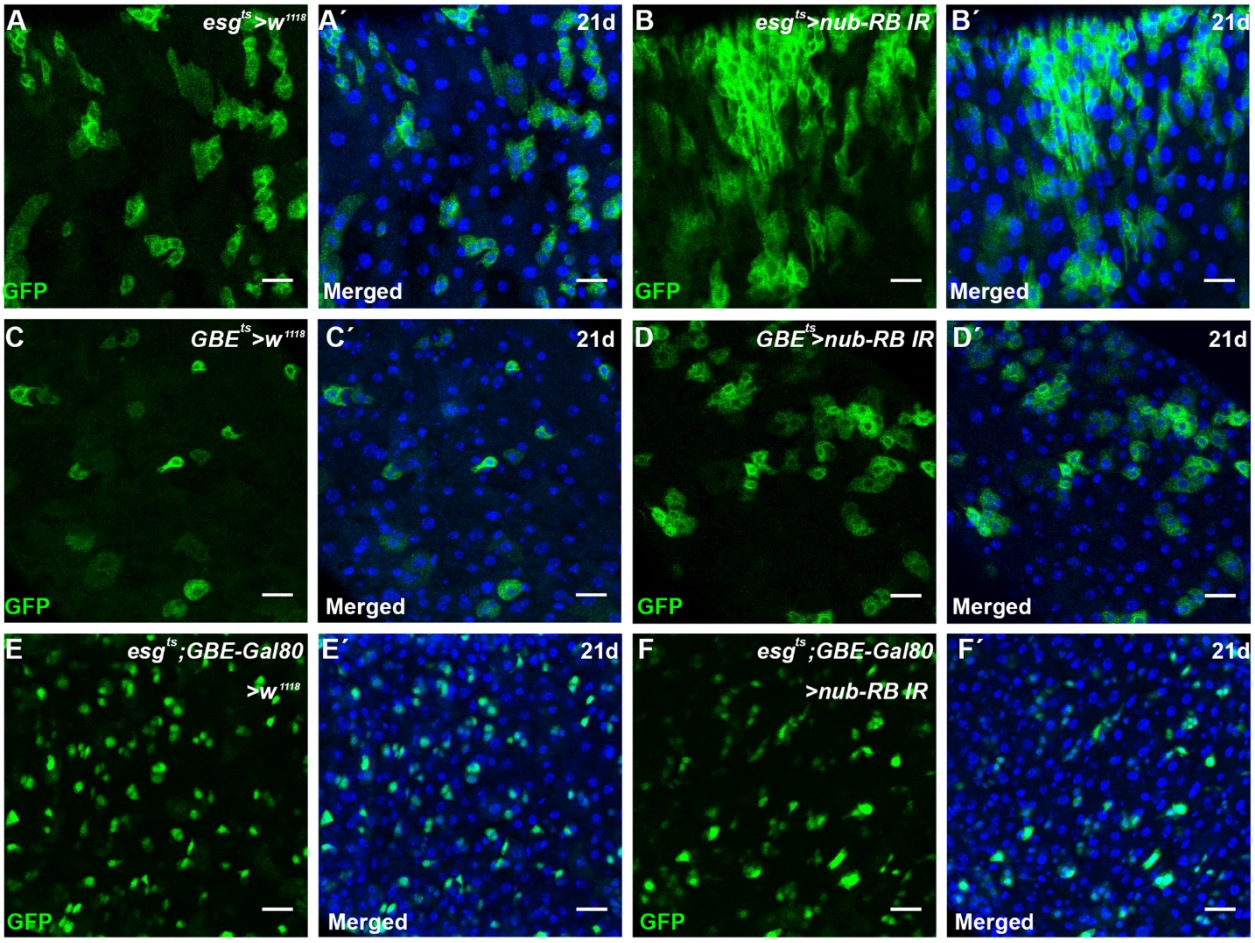

Figure S3. Function of Nub-PB in different cell types in posterior midgut. Related to Figure 4.

A-B´: Downregulation of *nub-RB* in progenitor cells (ISC+EB, GFP-labelled) using esg^{ts} for 21 days in posterior midgut. **C-D´**: Downregulation of *nub-RB* in EBs (GFP-labelled) using GBE^{ts} for 21 days in posterior midgut. **E-F´**: Downregulation of *nub-RB* in ISCs (GFP-labelled) using esg^{ts}*;GBE-Gal80* driver for 21 days in posterior midgut. Scale bars represent 20 µm.

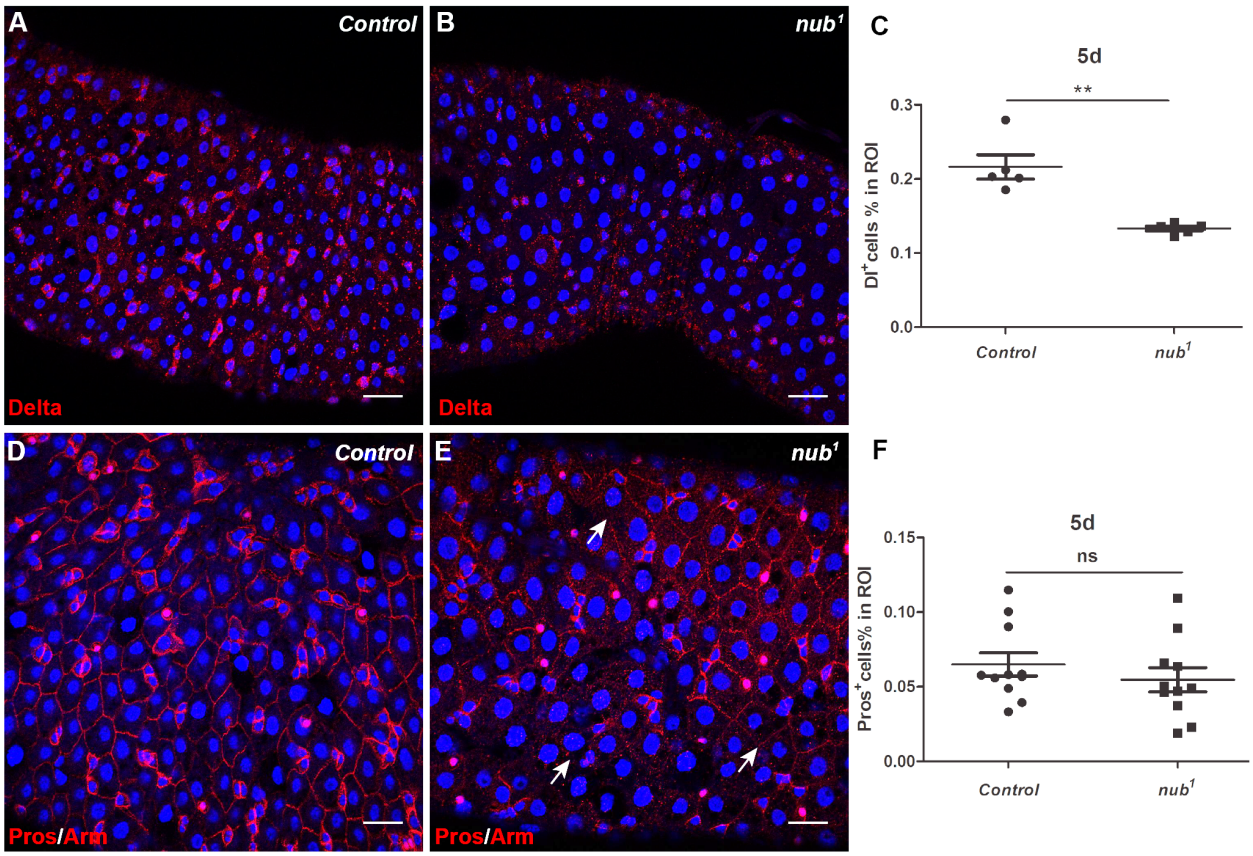

Figure S4. Low stem cell numbers and abnormal midgut epithelium arrangement in the *nub*^{1} mutant. Related to Figure 6.

A-B: Delta antibody staining in 5-day old posterior midguts of control (A, *n*=5) and *nub*^{1} (B, *n*=5). **C:** Quantification of the proportion of Delta positive stem cells in the R5 region. **D-E:** Arm and Pros antibody co-staining in 5-day old posterior midguts of control (D, *n*=11) and *nub*^{1} (E, *n*=11). **F:** Quantification of the proportion of Pros positive EE cells in R4 to R5 region. Statistical significance was calculated using unpaired t-test, ** $p<0.01$, ns: not significant. Error bars represent SEM. Scale bars represent 20 µm.

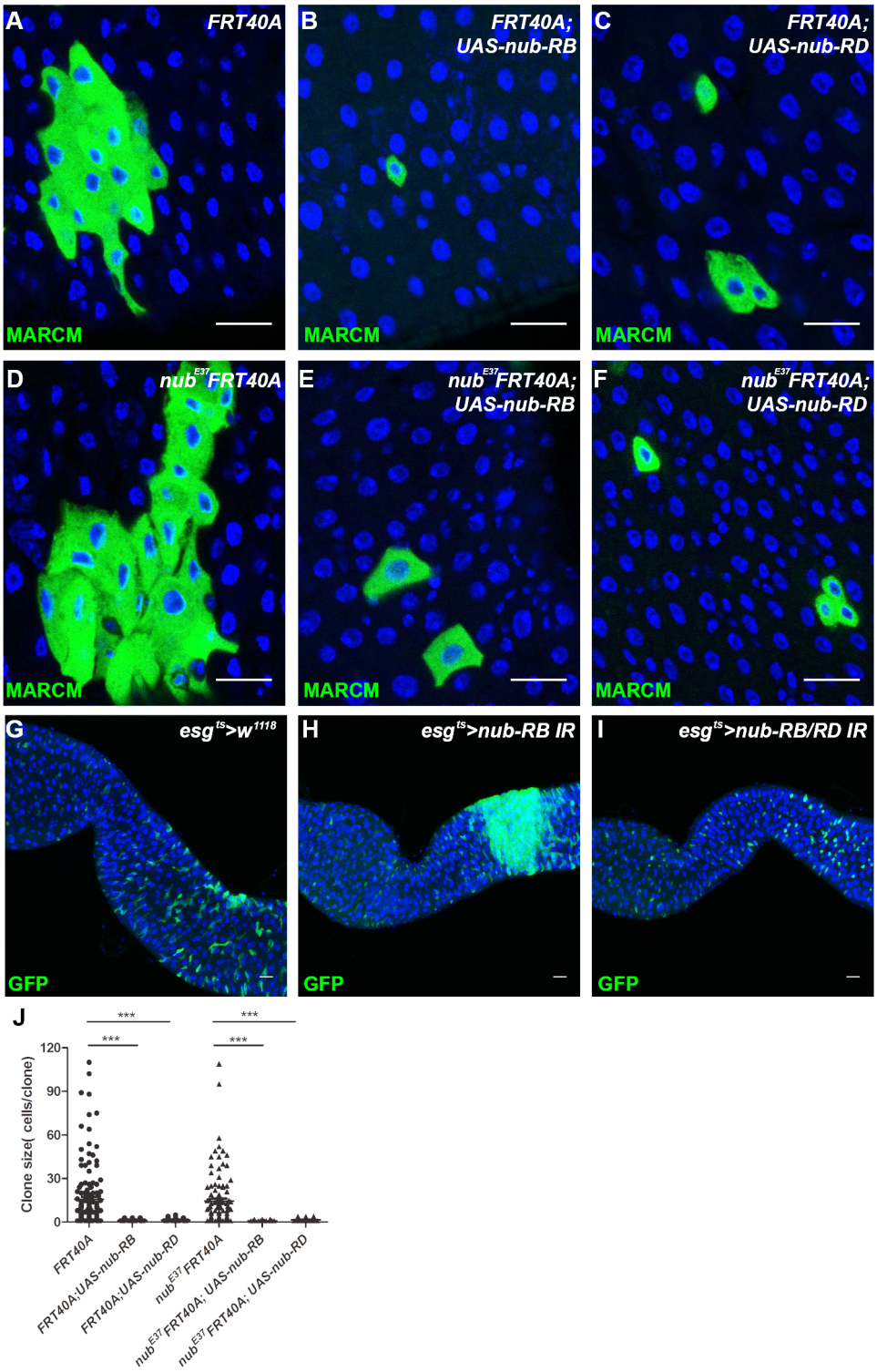
A
FRT40A
MARCM
B
FRT40A;
UAS-nub-RB
MARCM
C
FRT40A;
UAS-nub-RD
MARCM
D
nub E37 FRT40A
MARCM
E
nub E37 FRT40A;
UAS-nub-RB
MARCM
F
nub E37 FRT40A;
UAS-nub-RD
MARCM
G
esg ts >w 1118
GFP
H
esg ts >nub-RB IR
GFP
I
esg ts >nub-RB/RD IR
GFP
J
Clone size(cells/clone)
120
90
60
30
0
***
***
***
***
FRT40A
FRT40A;UAS-nub-RB
FRT40A;UAS-nub-RD
nub E37 FRT40A
nub E37 FRT40A; UAS-nub-RB
nub E37 FRT40A; UAS-nub-RD

Figure S5. MARCM analysis in different genetic background. Related to Figure 6.

A-C: MARCM clones with *nub-RB* (B) or *nub-RD* (C) overexpression in control (A) background. **D-F:** MARCM clones with *nub-RB* (E) or *nub-RD* (F) overexpression in nub^{E37} mutant (D) background. Note that A and D are re-use of Figure 6I and 6K respectively, included here for comparative purposes. **G-I:** Downregulation of *nub-RB alone* (H*) or both nub-RB and nub-RD* (I) in progenitor cells (ISC+EB, GFP-labelled) compared to control (G), using esg^{ts} for 10 days in posterior midgut (R4 region). **J:** Quantification of the number of cells in each MARCM clone. *n*=83 clones in B, *n*=84 clones in C, *n*=90 clones in E and *n*=85 clones in F. Statistical significance was calculated using one-way ANOVA, Tukey´s multiple comparisons test, ***$p<0.001$. Error bars represent SEM. Scale bars represent 20 µm.

2. Supplemental Experimental Procedures

Fly genotypes in related figures:

Figure 1: A*: w; FRT40A/FRT40A* (a gift from Heinrich Reichert)*, B: w; P[w+30A] nub^1 FRT40A/ P[w+30A] nub^1 FRT40A* (a gift from Wes Gruber)*, C: w; P[w+30A] nub^1 FRT40A / Nub^{E37} FRT40A* (a gift from Tetsuya Kojima)

Figure 2: A-A´´: *w; nub-RB-gal4/MyoIA-LacZ; UAS-mCherry/+*. B-B´´: *w; UAS-mCherry /MyoIA-LacZ; nub-RD-gal4 (VT006452)/+*. C-C´´:*w;nub-RB-gal4/GBE-Su[H]nlsGFP*(a gift from Joaquin de Navascues)*;UAS-mCherry/MKRS*. D-D´´:*w;UAS-mCherry/GBE-Su[H]nlsGFP; nub-RD-gal4/MKRS*. E-E´´: *w; esg-gal4; tubGal80ts,UAS-GFP*. F-G´´: *w; esg-LacZ/Cyo.*

Figure 3: A*: w; esg-gal4tubGal80ts UAS-GFP/+; UAS-flp act>CD2>gal4/+*. B: *w; esg-gal4tubGal80ts UAS-GFP/UAS-nub-RB; UAS-flp act>CD2>gal4/+*. C: *w; esg-gal4tubGal80ts UAS-GFP/UAS-nub-RB IR (VDRC105044); UAS-flp act>CD2>gal4/+*. D: *w; esg-gal4/+; tubGal80ts, UAS-GFP/+*. E: *w; esg-gal4/UAS-nub-RB; tubGal80ts, UAS-GFP/+*. F: *w; esg-gal4/UAS-nub-RBIR; tubGal80ts, UAS-GFP/+*. G: *w; esg-gal4/UAS-nub-RBIR; tubGal80ts, UAS-GFP/ UAS-esgIR (Bloomington28514).*

Figure 4: A-A´´´: *w; esg-gal4/+; tubGal80ts, UAS-GFP/+*. B-B´´´: *w; esg-gal4/UAS-nub-RBIR; tubGal80ts, UAS-GFP/+*. C-C´´´: *w; Su(H)GBE-gal4/+; tubGal80ts, UAS-GFP/+*. D-D´´´: *w; Su(H)GBE-gal4/UAS-nub-RBIR; tubGal80ts,UAS-GFP/+*. E: *w; esg-gal4, tubGal80ts UAS-YFP/+; Su(H)Gal80/+*. F: *w; esg-gal4, tubGal80ts UAS-YFP/UAS-nub-RBIR; Su(H)Gal80/+*.

Figure 5: A and E: *w; esg-gal4/+; tubGal80ts, UAS-GFP/+*. B and F: *w; esg-gal4/UAS-notchIR* (a gift from Ulrich Theopold /Artavanis-Tsakonas)*; tubGal80ts,UAS-GFP/+*. C and G: *w; esg-gal4/+; tubGal80ts,UAS-GFP/UAS-nub-RB*. D and H: *w; esg-gal4/UAS-notchIR; tubGal80ts, UAS-GFP/UAS-nub-RB.*

Figure 6: A: *Oregon-R*. B: *w; nub^1* (Dantoft et al.,2013). D and E: *w; FRT40A*. F and G: *w; P[w+30A] nub^1 FRT40A*. I: *yw, hsFlp[122]/+; FRT40A,tubGal80/FRT40A; tub-Gal4[LL7], UAS-GFP[LL6]/+;* J: *yw, hsFlp[122]/+; FRT40A,tub-Gal80/ P[w+30A] nub^1 FRT40A; tub-Gal4[LL7], UAS-GFP[LL6]/+;* K: *yw, hsFlp[122]/+; FRT40A,tub-Gal80/nub^{E37} FRT40A; tub-Gal4[LL7], UAS-GFP[LL6]/+*

Figure S1: A-A´´: *w; nub-RB-gal4/MyoIA-LacZ; UAS-mCherry/+*. B-B´´: *w; UAS-mCherry /MyoIA-LacZ; nub-RD-gal4/+*.

Figure S2: A-A´´: *yw, hsFlp[122]/+; FRT40A,tub-Gal80/ P[w+30A] nub^1 FRT40A; tub-Gal4[LL7], UAS-GFP[LL6]/+*.B-B´´: *yw, hsFlp[122]/+; FRT40A,tub-Gal80/nub^{E37} FRT40A; tub-Gal4[LL7], UAS-GFP[LL6]/+*.

Figure S3: A-A´: *w; esg-gal4/+; tubGal80ts, UAS-GFP/+*. B-B´: *w; esg-gal4/UAS-nub-RBIR; tubGal80ts, UAS-GFP/+*. C-C´: *w; Su(H)GBE-gal4/+; tubGal80ts, UAS-GFP/+*. D-D´: *w; Su(H)GBE-gal4/UAS-nub-RBIR; tubGal80ts,UAS-GFP/+*.E-E´: *w; esg-gal4, tubGal80ts UAS-YFP/+; Su(H)Gal80/+*. F-F´: *w; esg-gal4, tubGal80ts UAS-YFP/UAS-nub-RBIR; Su(H)Gal80/+*.

Figure S4: A and D: *Oregon-R*. B and E: *w; nub^1* (Dantoft et al.,2013).

Figure S5: A: *yw,hsFlp[122]/+; FRT40A,tub-Gal80/FRT40A; tub-Gal4[LL7], UAS-GFP[LL6]/+;* B: *yw, hsFlp[122]/+; FRT40A,tub-Gal80/FRT40A; tub-Gal4[LL7],UAS-GFP[LL6]/UAS-nub-RB;* C: *yw, hsFlp[122]/+; FRT40A,tub-Gal80/FRT40A; tub-Gal4[LL7], UAS-GFP[LL6]/UAS-nub-RD.* D: *yw, hsFlp[122]/+; FRT40A,tub-Gal80/nub^{E37}FRT40A; tub-Gal4[LL7],UAS-GFP[LL6]/+.* E: *yw, hsFlp[122]/+; FRT40A,tub-Gal80/ nub^{E37} FRT40A; tub-Gal4[LL7], UAS-GFP[LL6]/UAS-nub-RB.* F:*yw, hsFlp[122]/+; FRT40A,tub-Gal80/ nub^{E37} FRT40A; tub-Gal4[LL7], UAS-GFP[LL6]/UAS-nub-RD.* G: *w; esg-gal4/+; tubGal80ts, UAS-GFP/+*. H: *w; esg-gal4/UAS-nub-RBIR; tubGal80ts, UAS-GFP/+*. I: *w; esg-gal4/+; tubGal80ts, UAS-GFP/UAS-nub IR (VDRC6217).*

Immunostainings of *Drosophila* cell lines

Drosophila mbn-2 cells (Gateff et al., 1980) and S2 R^+ FUCCI cells (Zielke et al., 2014) were cultured in Schneider's cell medium (Gibco) supplemented with 10% fetal bovine serum (Gibco). 300 µl of a cell suspension (5 x 10^4 cells/ml) of mbn-2 or S2 R^+ FUCCI cells was applied into each µ-Slide 8 well plate (#80826, Ibidi) and cultivated at 25 °C incubator overnight. Cells were briefly washed with phosphate-buffered saline pH 7.4 (PBS) and fixed with 4% paraformaldehyde for 30 min at room temperature with gentle shaking. After blocking with PBST (0.1 % TritonX-100 in PBS) + 0.5% normal goat serum (NGS) for 30 min the cells were incubated with primary antibodies at 4 °C overnight. Next day, cells were washed with PBS, blocked again with PBST+0.5% NGS at RT for 30 min, then incubated with secondary antibodies for 2 h. Finally, cells were stained with DAPI (Sigma) and mounted with DABCO (Sigma) for imaging.

Antibodies and dilutions

Mouse anti-β-gal, 1:20 (Developmental Studies Hybridoma Bank, DSHB); Mouse anti-Pros, 1:100 (DSHB); Mouse anti-Delta, 1:100 (DSHB); Mouse anti-Arm, 1:300 (DSHB); Rabbit anti-Nub, 1:1500 (a gift from Bill Chia); Rabbit anti-PH3, 1:300 (06-570, MILLIPORE); Mouse anti- β-tubulin, 1:300 (E7, DSHB); Donkey anti-rabbit Alexa594, 1:700 (A11012, Invitrogen); Donkey anti-mouse Alexa594, 1:700 (A11005, Invitrogen); Donkey anti-mouse Alexa488, 1:700 (A21202, Invitrogen); Goat anti-rabbit Cy5, 1:1500 (A10523, Invitrogen)

Bacterial infection

Erwinia carotovora carotovora 15 (*Ecc15*) was kindly donated by Bruno Lemaitre and cultured in LB medium at 30 °C with shaking. Overnight cultures were pelleted and resuspended to OD 100 in a 1:1 ratio of bacterial medium and 1% isotonic phosphate-buffered saline PH7.4 (PBS). Prior to infection, flies were starved and desiccated in empty vials at 29 °C for 2 h, then fed with infectious solution (1:1 mixture of resuspended *Ecc15* and 5% sucrose) or mock solution (2.5% sucrose) at 29°C for 12 h.

MARCM clone induction

The *nub*^{1} FRT40A (a hypomorphic allele of *nub*, in which Nub-PD protein is not expressed) (Dantoft et al., 2013) and the *nub*^{E37} FRT40A (*nub*^{E37}is an EMS-induced protein null point allele of *nub*, in which neither Nub-PD nor Nub-PB are expressed) (Yeo et al.,1995) alleles were used for MARCM analysis. Newly eclosed male and female flies of appropriate genotypes were collected and kept together for at least four days. Flies (4-7 days old) were heat-shocked at 37 °C for 20 min to induce clones in the midgut. Then the flies were aged for 8 days before dissection and further analysis.

Midgut length measurement

Female intestines were dissected from appropriate genotypes, stained with DAPI (Sigma) and mounted in DABCO (Sigma). Overview images of each midgut were first taken under a 4x objective lens and then stitched by using Fiji software (Schindelin et al., 2012). All measurements were performed in microscope software ZEN2012 (ZEISS) under "graphics-line", and readouts were recorded as a pixel. Note that the midgut length was measured between the proventriculus and the midgut/hindgut junction.

3. Supplemental References

Gateff, E., Gissmann, L., Shrestha, R., Plus, N., Pfister, H., Schröder, J., and Zur Hausen, H. (1980). Characterization of two tumorous blood cell lines of Drosophila melanogaster and the viruses they contain. Invertebrate Systems in vitro, 517-533.

Schindelin, J., Arganda-Carreras, I., Frise, E., Kaynig, V., Longair, M., Pietzsch, T., Preibisch, S., Rueden, C., Saalfeld, S., Schmid, B.*, et al.* (2012). Fiji: an open-source platform for biological-image analysis. Nat Methods *9*, 676-682.